

for the complexes, and (c) the empirical energy function used in reasonable and well-balanced. The agreement with the experimental enthalpies and entropies of association is less quantitative, but the trend of increasing $-T\Delta S$ paralleling increasingly negative ΔH is observed in both experiment and theory. The relative electrostatic interaction energy is the key to the relative free energy of association for these molecules and the calculations have given qualitative insight (Figure 3) into why malononitrile interacts more strongly with 18-crown-6 than either nitromethane or acetonitrile. The trend in free energies cannot be explained by the relative dipole moments; rather the relative electrostatic potential gradient in the direction of the crown is the critical determinant. This ties in nicely with such an analysis for hydrogen bonding interactions.⁴²

Using the free energy perturbation approach, we have been able to calculate the relative free energies of association for malononitrile vs nitromethane and malononitrile vs acetonitrile to within experimental and calculational error. In this approach, unlike the molecular mechanics/normal mode method, dynamic effects are taken into account and many effects that are similar in both guests cancel; thus, it is not surprising that the agreement with experiment is more quantitative in the free energy perturbation approach. Nonetheless, it is encouraging that the agreement is so quantitative, given that a constraint had to be applied to prevent host/guest decomplexation during the simulations. These results further validate the power of the free energy method. The fact

that such agreement was achieved with no empirical adjustment of molecular mechanical parameters (standard atom types for van der Waals interactions and electrostatic potential derived charges) provides important validation of the robustness of this approach on this well-defined model system.

The following general question arises: when is the neglect of solvation energies justified in calculations such as those reported here? This approach is likely to work if the specific interactions between solutes and solute complexes with the solvent are weak. This is true for aliphatic hydrocarbon solvents with any neutral organic solute. For aromatic hydrocarbon solvents, such as benzene, neglect of solvation appears to be justified for solutes without proton donor functionality, such as studied here. The approach we have used is unlikely to work well for polar solvents and/or ionic solutes. Nonetheless, even in those cases it may be interesting to carry out the gas-phase simulations in order to quantitate and understand the solvation effect.

Acknowledgment. P.D.J.G. has been supported by a NATO Science Fellowship under the auspices of the Netherlands Organization for the Advancement of Pure Research (Z.W.O.). P.A.K. is pleased to acknowledge research support from the Institute of General Medical Sciences (GM-29072). The authors acknowledge the use of the UCSF Computer Graphics Laboratory facilities supported by grant RR-1081 to R. Langridge.

Registry No. 18-Crown-6/malononitrile, 63726-93-2; 18-crown-6/nitromethane, 82064-74-2; 18-crown-6/acetonitrile, 60336-83-6.

(42) Kollman, P. A. *J. Am. Chem. Soc.* **1977**, *99*, 4875-4894.

On the Thermal Behavior of Schiff Bases of Retinal and Its Analogues: 1,2-Dihydropyridine Formation via Six- π -Electron Electrocyclization of 13-Cis Isomers^{1a}

Angel R. de Lera,^{1b} Wolfgang Reischl,^{1c} and William H. Okamura*

Contribution from the Department of Chemistry, University of California, Riverside, California 92521. Received October 13, 1988

Abstract: Reaction of 13-*tert*-butyl-13-*cis*-retinal (**3a**) with *n*-butylamine affords *n*-butyl Schiff base **3b**, which affords the electrocyclic dihydropyridine (DHP) **7b** with a half-life of ~ 11 min at 23 °C in benzene-*d*₆. The corresponding 11,13-*dicis* Schiff base **5b** isomerizes to the same DHP-**7b** with a half-life of ~ 4 min at 78 °C. For *tert*-butyl Schiff bases 13-*cis*-**3c** and 11,13-*dicis*-**5c**, an equilibrium is established at 78 °C between **3c**, **5c**, and DHP-**7c** in a $\sim 5/2/3$ ratio, respectively. The parent 13-*cis*-retinal *n*-butyl Schiff base **2b** undergoes similar electrocyclization, but geometric isomerization occurs as a competing process. Because of the considerably more complex thermal behavior of the parent series, *n*-butyl and *tert*-butyl Schiff bases of aldehydes *all-trans*-**1a**, 13-*cis*-**2a**, and 9-*cis*-**11a** were prepared and then in parallel experiments subjected to thermal isomerization at 78 °C. For the *tert*-butyl Schiff bases **1c**, **2c**, and **11c**, only geometric isomerism leading to ~ 50 –60% of **1c**, near equal amounts ($\sim 20\%$ each) of **2c** and **11c**, and minor amounts (~ 6 –12%) of 9,13-*dicis*-**13c** occurs on prolonged heating. The *n*-butyl Schiff bases behave in a qualitatively similar manner except that 13-*cis*-**2b** produces significant amounts of DHP-**9b** and that in all cases prolonged heating leads to a myriad of minor components as indicated by ¹H NMR monitoring. For the seven-membered ring fused, 12-*s-cis*-locked series of *n*-butyl Schiff base analogues, 13-*cis*-**4b**, 11,13-*dicis*-**6b**, 9,11,13-*tricyclic*-**14b**, and 9,13-*dicis*-**16b**, similar thermal experiments were conducted, and the results resembled those of the 13-*tert*-butyl isomers 13-*cis*-**3b** and 11,13-*dicis*-**5b**, which are thought to be biased in 12-*s-cis* conformations. The remarkable facility with which 13-*cis* isomers of 13-*tert*-butyl and 12-*s-cis*-locked Schiff base analogues undergo electrocyclization to DHP's is attributed to their strongly biased or locked 12-*s-cis* conformations. Finally, it was shown that DHP-**7b**, which is formed exclusively when either 13-*cis*-**3b** or 11,13-*dicis*-**5b** is heated, is stable to prolonged heating (78 °C, 14 h) in benzene-*d*₆ and cannot be induced to undergo ring opening to protonated Schiff base **18** by protonation. Instead, protonation of DHP-**7b** afforded 2,3-dihydropyridinium salt **19**.

Schiff base derivatives of *all-trans*-(**1a**) and 13-*cis*-retinal (**2a**) (Chart I) with *n*-butylamine, namely, **1b** and **2b**, respectively, have been used extensively as models to reproduce the spectroscopic

and chemical properties of the several pigments of Halobacteria, particularly bacteriorhodopsin.² This pigment, which contains *all-trans*-retinal (**1a**) as chromophore bound to the ϵ -amino group of a lysine residue of the protein bacteriorhodopsin, functions as a

(1) (a) A preliminary account of this work has appeared: Okamura, W. H.; de Lera, A. R.; Reischl, W. *J. Am. Chem. Soc.* **1988**, *110*, 4462. (b) NATO Postdoctoral Fellow, 1985-1987. Present address: Department of Organic Chemistry, University of Santiago, Spain. (c) Present address: Department of Organic Chemistry, University of Vienna, Austria.

(2) (a) Stoeckenius, W. *Acc. Chem. Res.* **1980**, *13*, 337. (b) Stoeckenius, W.; Bogomolni, R. A. *Annu. Rev. Biochem.* **1982**, *52*, 587. (c) Oesterhelt, D. *Angew. Chem., Int. Ed. Engl.* **1976**, *15*, 17.

photochemical proton pump coupled to ATP synthesis. It is presently believed that light-induced *cis-trans* isomerization of the Δ^{13} double bond of the chromophore and protonation-deprotonation of the retinal Schiff base nitrogen are key processes involved in the proton pump photocycle.³⁻¹⁰ Useful information

(3) (a) Eisenstein, L.; Lin, S.-L.; Dollinger, G.; Odashima, K.; Termini, J.; Konno, K.; Ding, W.-D.; Nakanishi, K. *J. Am. Chem. Soc.* **1987**, *109*, 6860. (b) Dollinger, G.; Eisenstein, L.; Lin, S.-L.; Termini, J.; Nakanishi, K. *Biochemistry* **1986**, *25*, 6524. (c) Rao, V. J.; Derguini, F.; Nakanishi, K.; Taguchi, T.; Hosoda, A.; Hanzawa, Y.; Kobayashi, Y.; Pande, C. M.; Callender, R. H. *J. Am. Chem. Soc.* **1986**, *108*, 6077. (d) Derguini, F.; Dunn, D.; Eisenstein, L.; Nakanishi, K.; Odashima, K.; Rao, V. J.; Sastry, L.; Termini, J. *Pure Appl. Chem.* **1986**, *58*, 719. (e) Schiffmiller, R.; Callender, R. H.; Waddell, W. H.; Govindjee, R.; Ebrey, T. G.; Kakitani, H.; Honig, B.; Nakanishi, K. *Photochem. Photobiol.* **1985**, *41*, 563. (f) Chang, C. H.; Govindjee, R.; Ebrey, T.; Bagley, K. A.; Dollinger, G.; Eisenstein, L.; Marqu, J.; Roder, H.; Vittitow, J.; Fang, J.-M.; Nakanishi, K. *Biophys. J.* **1985**, *47*, 509. (g) Derguini, F.; Bigge, C. F.; Croteau, A. A.; Balogh-Nair, V.; Nakanishi, K. *Photochem. Photobiol.* **1984**, *39*, 661. (h) Fang, J.-M.; Carriker, J. D.; Balogh-Nair, V.; Nakanishi, K. *J. Am. Chem. Soc.* **1983**, *105*, 5162. (i) Sen, R.; Widlanski, T. S.; Balogh-Nair, V.; Nakanishi, K. *J. Am. Chem. Soc.* **1983**, *105*, 5160. (j) Sheves, M.; Nakanishi, K. *J. Am. Chem. Soc.* **1983**, *105*, 4033. (k) Kakitani, T.; Kakitani, H.; Honig, B.; Nakanishi, K. *J. Am. Chem. Soc.* **1983**, *105*, 648. (l) Derguini, F.; Caldwell, C. G.; Motto, M. G.; Balogh-Nair, V.; Nakanishi, K. *J. Am. Chem. Soc.* **1983**, *105*, 646. (m) Balogh-Nair, V.; Nakanishi, K. *Methods Enzymol.* **1982**, *88*, 496. (n) Motto, M. G.; Nakanishi, K. *Methods Enzymol.* **1982**, *88*, 178. (o) Balogh-Nair, V.; Carriker, J. D.; Honig, B.; Kamat, V.; Motto, M. G.; Nakanishi, K.; Sen, R.; Sheves, M.; Arnaboldi Tanis, M.; Tsujimoto, K. *Photochem. Photobiol.* **1981**, *33*, 483. (p) Motto, M. G.; Sheves, M.; Tsujimoto, K.; Balogh-Nair, V.; Nakanishi, K. *J. Am. Chem. Soc.* **1980**, *102*, 7947. (q) Nakanishi, K.; Balogh-Nair, V.; Arnaboldi, M.; Tsujimoto, K.; Honig, B. *J. Am. Chem. Soc.* **1980**, *102*, 7945.

(4) (a) Gerwert, K.; Siebert, F. *EMBO J.* **1986**, *5*, 805. (b) Tavan, P.; Schulten, K. *Biophys. J.* **1986**, *50*, 81.

(5) (a) Fodor, S. P. A.; Pollard, W. T.; Gebhard, R.; van den Berg, E. M. M.; Lugtenburg, J.; Mathies, R. A. *Proc. Natl. Acad. Sci. U.S.A.* **1988**, *85*, 2156. (b) Smith, S. O.; Braiman, M. S.; Myers, A. B.; Pardo, J. A.; Courtin, J. M. L.; Winkel, C.; Lugtenburg, J.; Mathies, R. A. *J. Am. Chem. Soc.* **1987**, *109*, 3108. (c) van der Steen, R.; Biesheuvel, P. L.; Mathies, R. A.; Lugtenburg, J. *J. Am. Chem. Soc.* **1986**, *108*, 6410. (d) Lugtenburg, J.; Muradin-Szweykowska, M.; Heeremans, C.; Pardo, J. A.; Harbison, G. S.; Herzfeld, J.; Griffin, R. G.; Smith, S. O.; Mathies, R. A. *J. Am. Chem. Soc.* **1986**, *108*, 3104. (e) Smith, S. O.; Hornung, I.; van der Steen, R.; Pardo, J. A.; Braiman, M. S.; Lugtenburg, J.; Mathies, R. A. *Proc. Natl. Acad. Sci. U.S.A.* **1986**, *83*, 967. (f) Harbison, G. S.; Mulder, P. P. J.; Pardo, J. A.; Lugtenburg, J.; Herzfeld, J.; Griffin, R. G. *J. Am. Chem. Soc.* **1985**, *107*, 4809. (g) Harbison, G. S.; Smith, S. O.; Pardo, J. A.; Courtin, J. M. L.; Lugtenburg, J.; Herzfeld, J.; Mathies, R. A.; Griffin, R. G. *Biochemistry* **1985**, *24*, 6955. (h) Harbison, G. S.; Smith, S. O.; Pardo, J. A.; Winkel, C.; Lugtenburg, J.; Herzfeld, J.; Mathies, R.; Griffin, R. G. *Proc. Natl. Acad. Sci. U.S.A.* **1984**, *81*, 1706. (i) Smith, S. O.; Myers, A. B.; Pardo, J. A.; Winkel, C.; Mulder, P. P. J.; Lugtenburg, J.; Mathies, R. *Proc. Natl. Acad. Sci. U.S.A.* **1984**, *81*, 2055. (j) Rothschild, K. J.; Roepe, P.; Lugtenburg, J.; Pardo, J. A. *Biochemistry* **1984**, *23*, 6103. (k) Harbison, G. S.; Smith, S. O.; Pardo, J. A.; Mulder, P. P. J.; Lugtenburg, J.; Herzfeld, J.; Mathies, R.; Griffin, R. G. *Biochemistry* **1984**, *23*, 2662.

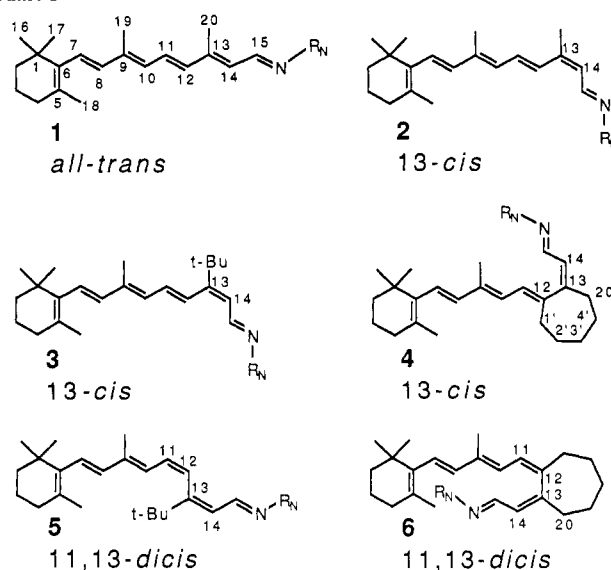
(6) (a) Cookingham, R. E.; Lewis, A.; Lemley, A. T. *Biochemistry* **1978**, *17*, 4699. (b) Marcus, M. A.; Lewis, A. *Biochemistry* **1978**, *17*, 4722. (c) Lewis, A.; Spoonhower, J. P.; Bogomolni, R. A.; Lozier, R. H.; Stoekenius, W. *Proc. Natl. Acad. Sci. U.S.A.* **1974**, *71*, 4462.

(7) (a) Seltzer, S.; Zuckermann, R. *J. Am. Chem. Soc.* **1985**, *107*, 5523. (b) Seltzer, S. *J. Am. Chem. Soc.* **1987**, *109*, 1627.

(8) (a) Baasov, T.; Friedman, N.; Sheves, M. *Biochemistry* **1987**, *26*, 3210. (b) Ghirlando, R.; Berman, E.; Baasov, T.; Sheves, M. *Magn. Reson. Chem.* **1987**, *25*, 21. (c) Albeck, A.; Friedman, N.; Sheves, M.; Ottolenghi, M. *J. Am. Chem. Soc.* **1986**, *108*, 4614. (d) Baasov, T.; Sheves, M. *Biochemistry* **1986**, *25*, 5249. (e) Sheves, M.; Friedman, N. *Angew. Chem., Int. Ed. Engl.* **1986**, *25*, 284. (f) Sheves, M.; Albeck, A.; Friedman, N.; Ottolenghi, M. *Proc. Natl. Acad. Sci. U.S.A.* **1986**, *83*, 3262. (g) Baasov, T.; Sheves, M. *J. Am. Chem. Soc.* **1985**, *107*, 7524. (h) Sheves, M.; Baasov, T. *J. Am. Chem. Soc.* **1984**, *106*, 6840. (i) Sheves, M.; Baasov, T.; Friedman, N.; Ottolenghi, M.; Feinmann-Weinberg, R.; Rosenbach, V.; Ehrenberg, B. *J. Am. Chem. Soc.* **1984**, *106*, 2435. (j) Sheves, M.; Rosenbach, V. *Chem. Lett.* **1984**, 525. (k) Sheves, M.; Friedman, N.; Rosenbach, V.; Ottolenghi, M. *FEBS Lett.* **1984**, *166*, 245. (l) Sheves, M.; Kohne, B.; Mazur, Y. *J. Chem. Soc., Chem. Commun.* **1983**, 1232. (m) Umadevi, P.; Sheves, M.; Rosenbach, V.; Ottolenghi, M. *Photochem. Photobiol.* **1983**, *38*, 197. (n) Sheves, M.; Baasov, T. *Tetrahedron Lett.* **1983**, *24*, 1745. (o) Sheves, M.; Baasov, T.; Friedman, N. *J. Chem. Soc., Chem. Commun.* **1983**, 77.

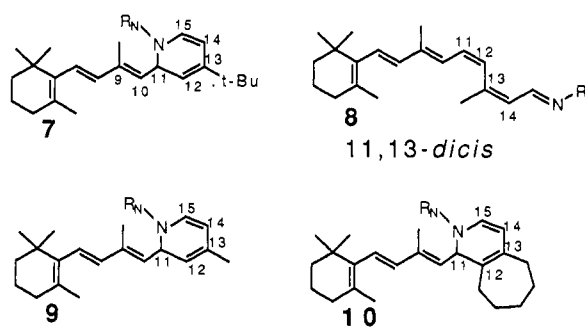
(9) Liu, R. S. H.; Mead, D.; Asato, A. E. *J. Am. Chem. Soc.* **1985**, *107*, 6609.

Chart I



a, $N-R_N = O$; b, $R_N = n\text{-Bu}$; c, $R_N = \text{tert-Bu}$

Chart II



a, $N-R_N = O$; b, $R_N = n\text{-Bu}$; c, $R_N = \text{tert-Bu}$

has been gleaned from studies involving Schiff base derivatives of retinal^{11,12} and its analogues.^{3,5,8-10,11e} For example, the di-

(10) (a) Kölling, E.; Oesterheld, D.; Hopf, H.; Krause, N. *Angew. Chem., Int. Ed. Engl.* **1987**, *26*, 580. (b) Ernst, L.; Hopf, H.; Krause, N. *J. Org. Chem.* **1987**, *52*, 398. (c) Gärtner, W.; Oesterheld, D.; Townner, P.; Hopf, H.; Ernst, L. *J. Am. Chem. Soc.* **1981**, *103*, 7642. (d) Gärtner, W.; Oesterheld, D.; Seifert-Schiller, E.; Townner, P.; Hopf, H.; Böhm, I. *J. Am. Chem. Soc.* **1984**, *106*, 5654.

(11) For optical studies of retinal Schiff base model systems, see besides ref 3d,e,m,o-q, 4, 5a,b, 6, and 8a,d,e,g,n,o: (a) Al-Dilaimi, S. K.; Aumiller, J. C.; Johnson, R. H.; Blatz, P. E. *Photochem. Photobiol.* **1987**, *46*, 403. (b) Blatz, P. E.; Mohler, J. H. *Biochemistry* **1975**, *14*, 2304. (c) Blatz, P. E.; Mohler, J. H.; Navangul, H. V.; *Biochemistry* **1972**, *11*, 848. (d) Blatz, P. E.; Mohler, J. H. *Biochemistry* **1972**, *11*, 3240. (e) Blatz, P. E.; Dewhurst, P. B.; Balasubramanian, V.; Balasubramanian, P.; Lin, M. *Photochem. Photobiol.* **1970**, *11*, 1. (f) Lukton, D.; Rando, R. R. *J. Am. Chem. Soc.* **1984**, *106*, 4525. (g) Lukton, D.; Rando, R. R. *J. Am. Chem. Soc.* **1984**, *106*, 258. (h) Rando, R. R.; Chang, A. J. *Am. Chem. Soc.* **1983**, *105*, 2879. (i) Mowery, P. C.; Stoekneius, W. *J. Am. Chem. Soc.* **1979**, *101*, 414. (j) Groenedijk, G. W. T.; Jacobs, C. W. M.; Bonting, S. L.; Daemen, F. J. M. *Eur. J. Biochem.* **1980**, *106*, 119. For closely related studies, see: Futterman, S.; Rollins, M. H. *J. Biol. Chem.* **1973**, *248*, 7773 and Futterman, A.; Futterman, S. *Biochim. Biophys. Acta* **1974**, *337*, 390. (k) Becker, R. S. *Photochem. Photobiol.* **1988**, *48*, 369. (l) Freedman, K. A.; Becker, R. S. *J. Am. Chem. Soc.* **1986**, *108*, 1245. (m) Becker, R. S.; Freedman, K. A. *J. Am. Chem. Soc.* **1985**, *107*, 1477. (n) Becker, R. S.; Freedman, K. A.; Causey, G. J. *Am. Chem. Soc.* **1982**, *104*, 5797. (o) Schaffer, A. M.; Waddell, W. H.; Becker, R. S. *J. Am. Chem. Soc.* **1974**, *96*, 2063. (p) López-Garriga, J. J.; Babcock, G. T.; Harrison, J. F. *J. Am. Chem. Soc.* **1986**, *108*, 7241. (q) López-Garriga, J. J.; Hanton, S.; Babcock, G. T.; Harrison, J. F. *J. Am. Chem. Soc.* **1986**, *108*, 7251. (r) López-Garriga, J. J.; Babcock, G. T.; Harrison, J. F. *J. Am. Chem. Soc.* **1986**, *108*, 7131. (s) Wingen, U.; Simon, L.; Klein, M.; Buss, V. *Angew. Chem., Int. Ed. Engl.* **1985**, *24*, 761. (t) Tabushi, I.; Shimokawa, K. *J. Am. Chem. Soc.* **1980**, *102*, 5400.

hydroretinals^{30-4,11c} allowed for the formulation^{3a} and later modification^{5d} of the point-charge model to explain the absorption characteristics of bacteriorhodopsin. Isotopically labeled retinals have provided a means for assigning the configurational and conformational characteristics of the retinal at the various intermediate stages of the photocycle.^{4,5} In addition, a number of other analogues have also been prepared to test some specific hypothesis or to provide additional structural or spectroscopic information.^{3,5,8-10,11c} In connection with this approach, we have prepared a number of retinal analogues modified at various positions of the side chain,¹³ and we recently initiated a systematic study of their Schiff base derivatives.^{1a} Initial studies indicated the extraordinarily facile thermal six-electron electrocyclicization¹⁴ processes characteristic of *n*-butyl and *tert*-butyl Schiff base derivatives of certain retinal analogues¹⁵ such as 3-6.^{1a} It is the purpose of this article to provide a full account of the preliminary communication^{1a} as well as to report on new, more detailed results concerning the behavior of Schiff bases of the retinals possessing a 13-*cis* configuration (e.g., 2, 3, and 5) and 12-*s-cis*-biased (e.g., 3) or -locked (e.g., 4) conformations. Related studies of other geometric isomers are also included with this report.

It has recently been shown that high-field NMR spectroscopy is a reliable method for directly analyzing the mixture of retinylidene iminium salts (protonated Schiff bases), thus avoiding the need for hydrolysis to the retinals and subsequent examination of the retinal composition after HPLC separation.^{12a,b} For these protonated Schiff bases, formation of the oximes followed by HPLC separation is reportedly useful because this process maintains geometric integrity.^{11f-h} This derivatization process however gives a syn-anti mixture of isomeric oximes, and the composition of the mixture of retinals has to be calculated with adequate correction of the molar absorptivity of the oximes by examination of the HPLC trace.^{11j} As in the recent studies by Childs^{12a,b} and Sheves,^{8b,h} we also considered high-field NMR to be a more direct method for analyzing the isomeric composition of Schiff bases of retinal isomers. Of course, a requisite was that samples of well-characterized substrates be available for direct spectroscopic comparisons. The advantage is that the course of a particular reaction can be monitored directly by NMR spec-

troscopy and the interconversion of Schiff bases could also be followed kinetically.

The choice of *n*-butylamine Schiff base derivatives for study seems well justified as a chemical model for the pigment bacteriorhodopsin in light of the fact that retinal is bound to the protein via a lysine residue (*vide supra*). The studies directed toward developing an understanding of the processes that operate with a Schiff base and its protonated counterpart render side by side studies of the *tert*-butylamine-derived Schiff bases^{8h,12a,b,e} a useful complement to the *n*-butylamine Schiff base studies. The bulky *tert*-butyl group renders the terminal carbon-nitrogen double bond (Δ^{15}) strongly if not exclusively *trans*, thus simplifying spectral interpretation.

Results and Discussion

The preparation of the Schiff bases was initially carried out according to conditions¹⁶ consisting of reacting the retinal with a 5-fold excess of the amine in ethanol containing molecular sieves at 0 °C for 1 h. The solid was removed by filtration, and the solvent was removed under vacuum for an additional 1 h at room temperature (method A). In subsequent experiments with the parent system, we found that 13-*cis*-retinal (2a) is converted within 10 min to the *n*-butyl Schiff base 2b in a variety of solvents (ethanol, ether, etc. with molecular sieves) with either 1.1 or 5 molar equiv of *n*-butylamine at 0 °C. After filtration, concentration of the reaction solution under a good vacuum afforded the residual Schiff base within a time period of about ~20 min (method B). The *n*-butyl Schiff base of 13-*tert*-butyl-13-*cis*-retinal (3b) could also be prepared in this manner. However, the *all-trans*-retinal *n*-butyl Schiff base (1b) and all the *tert*-butylamine-derived Schiff bases had to be prepared with method A because of incomplete formation of Schiff base. As expeditiously as possible following sample preparation using method A or B, the residue was dissolved in an appropriate solvent, and the composition of the product was monitored by high-field NMR (300 MHz) analysis (and/or by examination of the UV-vis absorption spectrum). The choice of the solvent is critical due to the long time course of some of the thermolysis reactions. It was necessary to find a relatively inert solvent with a conveniently high boiling point. As also reported by Rando,^{11f} it became clear that CDCl₃ was too reactive toward Schiff bases to be suitable for some of the thermal studies. While the less reactive CD₂Cl₂ has been successfully used with retinal Schiff bases and iminium salts, benzene-*d*₆ proved to be more suitable because of its higher boiling point. Accordingly, most experiments reported herein were conducted in the latter solvent. Tables I (C₆D₆) and II (CDCl₃) summarize the ¹H NMR data for the *n*-butyl and *tert*-butyl Schiff bases (2-6) studied. Details of the chemical reactivity and properties of the different Schiff bases are given below.

Schiff Bases of 13-*tert*-Butyl-13-*cis*-retinal (3a) and 13-*tert*-Butyl-11,13-*dicis*-retinal (5a). Under the standard conditions of method A, the reaction of 13-*tert*-butyl-13-*cis*-retinal (3a) with *n*-butylamine did not afford the expected Schiff base 3b. Instead, the heterocycle 1,2-dihydropyridine (DHP) 7b was formed (Chart II). A related heterocycle, the dihydropyran 9a, was previously postulated as a reactive intermediate via electrocyclicization in the isomerization of the parent 11,13-*dicis*-retinal (8a) to 13-*cis*-retinal (2a).¹³ⁱ Since 13-*cis* aldehyde 3a can be synthesized by thermal rearrangement of 11,13-*dicis* aldehyde 5a,^{13a,b} presumably via the intermediacy of α -dihydropyran 7a, the formation of 7b in retrospect comes as no surprise except for the unexpectedly mild conditions under which cyclization occurred¹⁷ and the thermodynamic features of these processes (i.e., the aldehyde prefers to exist in the open form while its Schiff base prefers the cyclic DHP

(12) For NMR studies of retinal Schiff base model systems, see besides ref 5f-h,k and 8b,h: (a) Childs, R. F.; Shaw, G. S. *J. Am. Chem. Soc.* **1988**, *110*, 3013. (b) Childs, R. F.; Shaw, G. S.; Wasylshen, R. E. *J. Am. Chem. Soc.* **1987**, *109*, 5362. (c) Birge, R. R.; Murray, L. P.; Zidovetzki, R.; Knapp, H. M. *J. Am. Chem. Soc.* **1987**, *109*, 2090. (d) Cossette, D.; Vocelle, D. *Can. J. Chem.* **1987**, *65*, 661. (e) Cossette, D.; Vocelle, D. *Can. J. Chem.* **1987**, *65*, 1576. (f) Pattaroni, C.; Lauterwein, J. *Helv. Chim. Acta* **1981**, *64*, 1969. (g) Sharma, G. M.; Roels, O. A. *J. Org. Chem.* **1973**, *38*, 3648. (h) Inoue, Y.; Tokito, Y.; Tomonoh, S.; Chujo, R. *Bull. Chem. Soc. Jpn.* **1979**, *52*, 265. (i) Inoue, Y.; Tokito, Y.; Chujo, R.; Miyoshi, Y. *J. Am. Chem. Soc.* **1977**, *99*, 5592.

(13) (a) Norman, T. C.; de Lera, A. R.; Okamura, W. H. *Tetrahedron Lett.* **1988**, *29*, 1251. (b) de Lera, A. R.; Okamura, W. H. *Tetrahedron Lett.* **1987**, *28*, 2921. (c) Shen, G.-Y.; de Lera, A. R.; Norman, T. C.; Haces, A.; Okamura, W. H. *Tetrahedron Lett.* **1987**, *28*, 2917. (d) Silveira, M. H.; Okamura, W. H. *J. Org. Chem.* **1985**, *50*, 2390. (e) Chauhan, Y. S.; Chandraratna, R. A. S.; Miller, D. A.; Kondrat, R. W.; Reischl, W.; Okamura, W. H. *J. Am. Chem. Soc.* **1985**, *107*, 1028. (f) Chandraratna, R. A. S.; Birge, R. R.; Okamura, W. H. *Tetrahedron Lett.* **1984**, *25*, 1007. (g) Chandraratna, R. A. S.; Okamura, W. H. *Tetrahedron Lett.* **1984**, *25*, 1003. (h) Chandraratna, R. A. S.; Bayerque, A. L.; Okamura, W. H. *J. Am. Chem. Soc.* **1983**, *105*, 3588. (i) Knudsen, C. G.; Chandraratna, R. A. S.; Walkeapää, L. P.; Chauhan, Y. S.; Carey, S. C.; Cooper, T. M.; Birge, R. R.; Okamura, W. H. *J. Am. Chem. Soc.* **1983**, *105*, 1626. (j) Okamura, W. H. *Acc. Chem. Res.* **1983**, *16*, 81. (k) Chandraratna, R. A. S.; Okamura, W. H. *J. Am. Chem. Soc.* **1982**, *104*, 6114. (l) Knudsen, C. G.; Carey, S. C.; Okamura, W. H. *J. Am. Chem. Soc.* **1980**, *102*, 6355. (m) Sueiras, J.; Okamura, W. H. *J. Am. Chem. Soc.* **1980**, *102*, 6255.

(14) (a) Marvell, E. N. *Thermal Electrocyclic Reactions*; Academic Press: New York, 1980. (b) Marvell, E. N.; Caple, G.; Schatz, B.; Pippin, W. *Tetrahedron* **1973**, *29*, 3781. (c) Marvell, E. N.; Seubert, J. *J. Am. Chem. Soc.* **1967**, *89*, 3377. (d) Huisgen, R.; Dahmen, A.; Huber, H. *J. Am. Chem. Soc.* **1967**, *89*, 7130.

(15) The carbons of retinal analogues are numbered with reference to the parent system (as in Chart I). To minimize confusion resulting from substituent priority rule changes, geometries are also designated in reference to the parent system ("cis" and "trans" rather than *Z* and *E*, respectively, are used throughout). Note that throughout this article, the **a** series refers to the aldehyde (R_N-N = oxygen), and the **b** and **c** series refer to the *n*-butyl (R_N = *n*-Bu) and *tert*-butyl (R_N = *tert*-Bu) Schiff base derivatives, respectively.

(16) The method for preparing Schiff base derivatives used in this study is a collective variation of previously reported methods. For example, see ref 8b and 12 for leading references.

(17) Electrocyclization of (3Z)-1,3,5-hexatriene derivatives in the carbocyclic series typically requires temperatures of >100 °C. See pp 269-271 in ref 14a for a review. The finding that DHP's are formed so readily may be understood in terms of a steric effect and/or the phenomenon referred to as pseudoelectrocyclization. See Okamura, W. H.; Peter, R.; Reischl, W. *J. Am. Chem. Soc.* **1985**, *107*, 1034, and ref 44-45 cited therein.

Table I. ¹H NMR Spectral Data for the Schiff Bases (C₆D₆)^{a,b}

	H ₇	H ₈	H ₁₀	H ₁₁	H ₁₂	H ₁₄	H ₁₅	C _{16,17} - 2CH ₃	C ₁₈ - CH ₃	C ₁₉ - CH ₃	C ₂₀ - CH ₃	C ₂₀ - tBu	H ₁ ^c	H ₄ ^c	N- tBu
1b	6.31	6.31	6.10	6.78	6.30	6.56	8.25	1.13	1.79*	1.82*	1.86*		3.51	0.91	
			(11.3)	(15.0, 11.4)	(15.0)	(9.3)	(9.3)						(t, 6.6)	(t, 7.2)	
1c	6.31	6.31	6.10	6.79	6.33	6.61	8.37	1.14	1.79*	1.86*	1.87*				1.25
			(11.4)	(15.3, 11.4)	(15.3)	(9.1)	(9.1)								
2b^d	6.39	6.39	6.26	6.78	7.06	6.41	8.52	1.18	1.83*	1.85*	1.89*		3.55	0.95	
			(11.2)	(14.7, 11.2)	(14.7)	(9.3)	(9.3)						(t, 6.6)	(t, 7.5)	
2c	6.33	6.33	6.22	6.76	7.13	6.44	8.61	1.13	1.80	1.81	1.85				1.24
			(11.4)	(15.1, 11.3)	(15.1)	(9.3)	(9.3)			(0.9)					
3b^d	6.28	6.28	obs ^c	6.73	obs ^c	6.61	8.4	1.11	1.76*	1.79*		1.00	3.50	0.86	
				(14.3, 12.0)		(8.5)	(br)	1.09					(t, 6.6)	(t, 7.7)	
3c^d	6.31	6.31	6.19	6.76	6.21	6.64	8.48	1.11	1.78	1.83		1.04			1.26
			(11.5)	(14.9, 11.5)	(14.9)	(8.5)	(8.5)								
4b	6.33	6.41	6.46	6.61		6.51	8.40	1.16	1.81	1.91			3.52	0.93	
	(16.8)	(16.8)	(12.6)	(12.6)		(8.0)	(8.0)						(t, 6.5)	(t, 6.5)	
4c	6.33	6.40	6.48	6.64		6.53	8.50	1.16	1.80	1.93					1.30
	(16.2)	(16.2)	(12.0)	(12.0)		(8.7)	(8.7)								
5b	6.29	6.20	5.95	6.62	6.37	6.60	8.16	1.06	1.67	1.85		1.01	3.45	0.87	
	(16.1)	(16.1)	(11.6)	(11.6, 11.6)	(11.6)	(8.7)	(8.7)						(t, 6.8)	(t, 7.6)	
5c	6.26	6.14	5.97	6.61	6.28	6.63	8.14	1.06	1.64	1.84		1.03			1.25
	(16.2)	(16.2)	(11.7)	(11.7, 11.7)	(11.7)	(8.5)	(8.5)								
6b	6.26	6.27	6.38	6.50		6.49	8.11	1.12	1.73	1.93			3.45	0.90	
			(11.7)	(11.7)		(9.1)	(9.1)						(m)	(m)	
6c	6.29	6.21	6.34	6.54		6.54	8.14	1.12	1.72	1.94					1.27
	(16.4)	(16.4)	(11.7)	(11.7)		(8.7)	(8.7)	1.13							
11b	6.35	6.98	5.98	7.04	6.26	6.54	8.20	1.11	1.74	1.81	1.90		3.47	0.90	
	(16.0)	(16.0)	(11.4)	(15.1, 11.4)	(15.1)	(9.4)	(9.4)						(t, 6.6)	(t, 7.2)	
11c	6.34	6.99	5.97	7.05	6.30	6.59	8.31	1.11	1.80	1.80	1.91				1.22
	(15.9)	(15.9)	(11.4)	(14.9, 11.4)	(14.9)	(9.1)	(9.1)								
12b	6.30	6.30	5.89	6.38	6.83	6.66	8.18	1.08	1.70	1.80	1.92		3.46	0.89	
			(12.0)	(12.0, 12.0)	(12.0)	(9.1)	(9.1)						(t, 6.6)	(t, 7.5)	
12c	6.31	6.25	5.91	6.38	6.85	6.69	8.30	1.08	1.69	1.81	1.96				1.21
	(15.9)	(15.9)	(12.0)	(12.0, 12.0)	(12.1)	(9.0)	(9.0)								

^a Refer to the figures in the text. The numbering and geometry notations are based on standard retinoid nomenclature irrespective of changes in group priorities in analogues. Except as noted, values in parentheses are doublet or double doublet splittings; δ values are not parenthesized and are singlets unless followed by parentheses. ^b Those assignments indicated by an asterisk (*) along any row may be reversed. ^c These refer to the *n*-butylamine side chain. ^d These substances were accompanied by varying amounts of the corresponding dihydropyridine (see Table III).

Table II. ¹H NMR Spectral Data for the Schiff Bases (CDCl₃)^{a,b}

	H ₇	H ₈	H ₁₀	H ₁₁	H ₁₂	H ₁₄	H ₁₅	C _{16,17} - 2CH ₃	C ₁₈ - CH ₃	C ₁₉ - CH ₃	C ₂₀ - CH ₃	C ₂₀ - tBu	H ₁ ^c	H ₄ ^c	N- tBu
1b	6.24	6.14	6.16	6.84	6.37	6.21	8.31	1.04	1.72	1.99	2.10		3.51	0.94	
	(16.1)	(16.1)	(11.4)	(15.1, 11.4)	(15.1)	(9.6)	(9.6)						(t, 7.0)	(t, 7.0)	
1c	6.23	6.14	6.22	6.84	6.37	6.16	8.33	1.03	1.72	1.99	2.10				1.25
	(16.1)	(16.1)	(11.5)	(15.1, 11.5)	(15.1)	(9.4)	(9.4)				(0.8)				
2b^d	6.26	6.14	6.19	6.79	6.97	6.07	8.45	1.04	1.72	2.00	2.05		3.49	0.94	
	(16.2)	(16.2)	(11.3)	(14.9, 11.3)	(14.9)	(9.5)	(9.5)						(t, 6.9)	(t, 7.0)	
2c	6.26	6.15	6.21	6.79	6.97	6.11	8.48	1.04	1.73	2.00	2.06				1.25
	(16.3)	(16.3)	(11.2)	(14.9, 11.2)	(14.9)	(9.7)	(9.7)				(0.7)				
3c	6.24	6.13	6.15	6.60	6.20	6.25	8.23	1.04	1.74	1.93		1.14			1.23
	(16.1)	(16.1)	(11.2)	(14.9, 11.2)	(14.9)	(8.7)	(8.7)								
4b^d	6.24	6.17	6.29*	6.34*		6.10	8.06	1.03	1.74	1.93			3.42	0.92	
	(16.3)	(16.3)	(12.0)	(12.0)		(9.1)	(9.1)						(t, 6.7)	(t, 6.5)	
4c	6.19	6.19	6.28*	6.34*		6.13	8.15	1.05	1.74	1.92					1.20
			(12.0)	(12.0)		(8.9)	(8.9)								
5b^d	6.17	6.03	6.00	6.70	6.03	6.21	7.85	1.01	1.68	1.96		1.13	3.34	0.86	
	(15.8)	(15.8)	(11.6)	(11.6, 11.6)	(11.6)	(8.9)	(8.9)	1.05					(t, 7.0)	(t, 7.0)	
5c^d	6.17	6.01	5.95	6.71	6.07	6.24	7.87	0.99	1.66	1.95		1.10			1.14
	(16.4)	(16.4)	(11.6)	(11.6, 11.6)	(11.6)	(8.7)	(8.7)								
6b^d	6.07	6.02	5.95	6.41		6.13	7.76	1.00	1.68	1.93			3.34	0.86	
	(15.3)	(15.3)	(11.6)	(11.6)		(9.5)	(9.5)	1.01					(m)	(t, 7.5)	
6c	6.18	6.07	6.10	6.52		6.25	7.84	1.05	1.73	2.00					1.17
	(16.5)	(16.5)	(11.5)	(11.5)		(9.0)	(9.0)	1.07							

^a Refer to the charts in the text. The numbering and geometry notations are based on standard retinoid nomenclature irrespective of changes in group priorities in analogues. Except as noted, values in parentheses are doublet or double-doublet splittings; δ values are not parenthesized and are singlets unless followed by parentheses.

^b Those assignments indicated by an asterisk (*) along any row may be reversed. ^c These refer to the *n*-butylamine side chain. ^d These substances were contaminated by varying amounts of the corresponding dihydropyridine (see Table III). The parent **2b** was also contaminated by **1b**.

form; vide infra).¹⁸ The analogous ring-fused oxa cycle **10a** was also considered to intercede in the equilibration of 11,13-*dicis*-**6a** and 13-*cis*-**4a**.^{13g} In point of fact, the geometric isomerization via thermal ring closure–ring opening electrocyclization of the γ,δ double bond of α,β -*cis*-dienals appears to have had its earliest precedent in the studies by Kluge and Lillya.¹⁹ In the nitrogen heterocycle series, *cis*-dienone oximes are known to form pyridines, presumably via electrocyclization followed by dehydration.²⁰ Also,

N-acyl-1,2-dihydropyridines have been obtained by electrocyclic ring closure of *N*-acylazatrienes, but the latter were generated at 650 °C under flash vacuum pyrolysis conditions so that the facility of the six- π -electron electrocyclization process was masked.²¹ Thus, in view of these mechanistic precedents, DHP-**7b** formation via electrocyclization of the putative Schiff base **3b** was logical, and the spectral data, particularly its ¹H NMR spectrum (Figure 1 and Table III), were in accord with the assignment.

Using method B for reacting *n*-butylamine with **3a** provided a convenient means for directly monitoring the formation of **3b**

(18) Some α,β -*cis*-dienals do exist mainly as the α -dihydropyran valence tautomer however. See pp 305–321 in ref 14a for a review.

(19) (a) Kluge, A. F.; Lillya, C. P. *J. Am. Chem. Soc.* **1971**, *93*, 4458. (b) Kluge, A. F.; Lillya, C. P. *J. Org. Chem.* **1971**, *36*, 1977, 1988.

(20) (a) Schiess, P.; Chia, H. L.; Ringe, P. *Tetrahedron Lett.* **1972**, 313. (b) See also Baran, J.; Mayr, H. *J. Am. Chem. Soc.* **1987**, *109*, 6519.

(21) (a) Cheng, Y.-S.; Lupo, A. T., Jr.; Fowler, F. W. *J. Am. Chem. Soc.* **1983**, *105*, 7696. (b) Wyle, M. J.; Fowler, F. W. *J. Org. Chem.* **1984**, *49*, 4025.

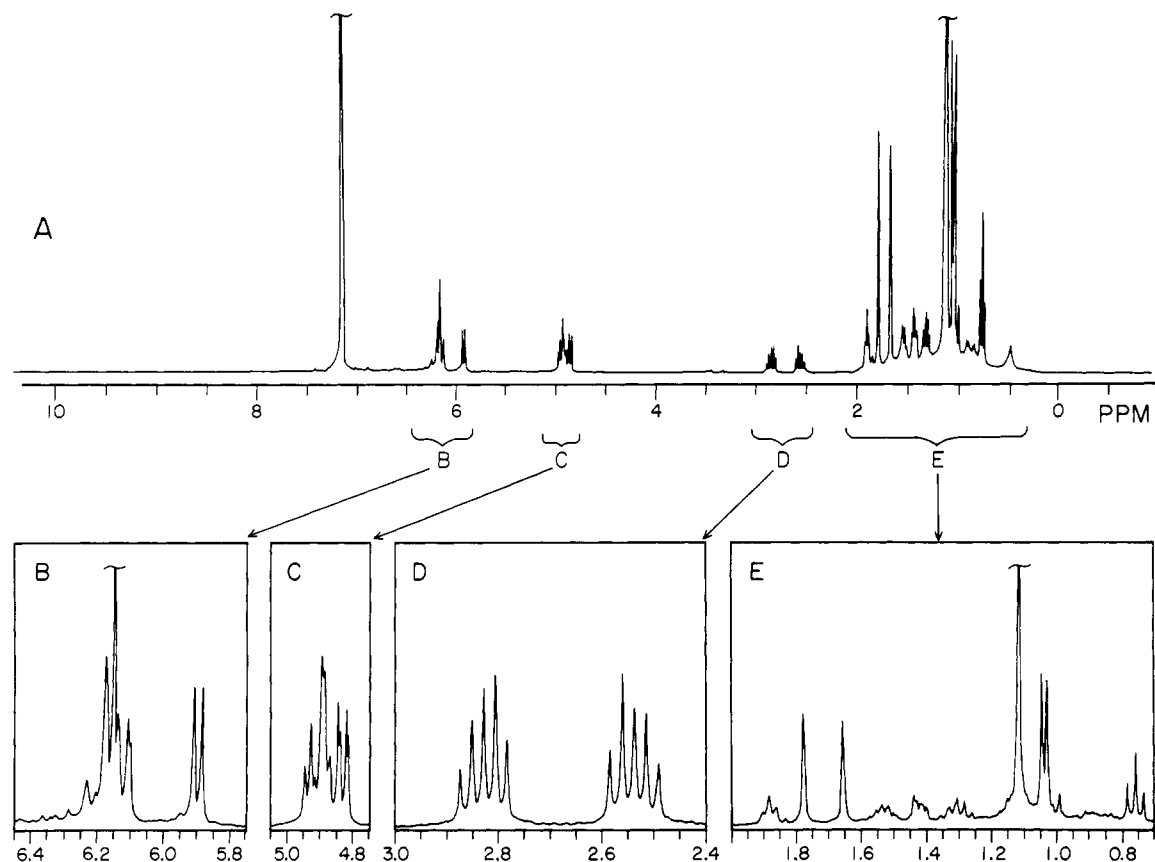


Figure 1. ^1H NMR spectrum at 300 MHz (residual protio C_6D_6 , δ 7.16) of 1,2-dihydropyridine (DHP) **7b** in C_6D_6 . Particularly diagnostic of the formation of *n*-butylamine-derived DHP's is the appearance of a pair of doublet of triplet signals in the region δ 2.4–3.0 assignable to the diastereotopic hydrogens of the α -methylene group next to nitrogen of the *n*-butyl group. The spectrum remains essentially unchanged after prolonged heating (78 $^\circ\text{C}$, 14 h). Additional details are presented in Table III and under Experimental Section.

Table III. ^1H NMR Spectral Data for the 1,2-Dihydropyridines (DHP)^{a,b}

	H_7	H_8	H_{10}	H_{11}	H_{12}	H_{14}	H_{15}	$\text{C}_{16,17}$ 2 CH_3	C_{18} CH_3	C_{19} CH_3	C_{20} CH_3	C_{20} <i>t</i> Bu	$\text{H}_{1'a}$ ^c	$\text{H}_{1'b}$ ^c	H_4 ^c	N- <i>t</i> Bu
CDCl₃																
7b	6.04 (16.0)	6.00 (16.0)	5.76 (9.4)	4.82 (9.4, 4.7)	4.65 (4.7, 2.0)	4.63 (7.6, 2.0)	5.98 (7.6)	1.019 1.022	1.70 1.10	1.81 1.95		1.03 1.16	2.95 (13.8, 7.4, 6.5)	2.76 (13.8, 7.5, 6.4)	0.89 (t, 7.3)	
7c^d	obsc	obsc	5.95 (9.2)	4.86 (9.2, 6.1)	4.71 (6.1, 2.0)	4.82 (7.6, 2.0)	obsc									1.25
9b^d	obsc	obsc	5.78 (9.0)	4.80 (9.0, 4.5)	4.65 (4.5)	4.45 (7.5, 2.2)	5.97 (7.5)	1.02	1.68	1.81	obsc		2.99 (14.0, 6.7, 6.7)	2.81 (14.0, 6.7, 6.7)	obsc	
10b	6.09 (16.2)	6.00 (16.2)	5.82 (7.0)	4.45 (7.0)		4.54 (10.0)	5.76 (10.0)	1.03	1.70	1.86			2.93 (14.0, 7.2, 6.6)	2.77 (14.0, 7.2, 6.6)	0.90 (t, 7.0)	
C₆D₆																
7b	6.20 (16.2)	6.13 (16.2)	6.12 (8.2)	4.89 (8.2, 5.1)	4.93 (5.1, 1.9)	4.82 (7.5, 1.9)	5.90 (7.5)	1.03 1.04	1.65* 1.10	1.77* 1.81		1.14 1.02	2.82 (13.6, 6.9, 6.8)	2.53 (13.6, 6.9, 6.8)	0.76 (t, 7.0)	
7c^d	obsc	obsc	obsc	5.07 (7.2)	4.95 (6.0, 0.9)	4.95 (m)	obsc	1.10 1.14	1.65	1.81						1.25
9b^d	obsc	obsc	obsc	4.91 (8.9, 4.5)	4.81 (4.5)	4.70 (7.0, 1.8)	5.89 (7.0)	1.12	1.74*	1.77*	1.80*		2.88 (13.9, 6.7, 6.7)	2.58 (13.9, 6.7, 6.7)	obsc	
10b	6.29 (16.0)	6.21 (16.0)	5.80 (7.0)	4.77 (7.0)		4.69 (9.8)	6.19 (9.8)	1.13	1.75	1.90			2.90 (14.0, 7.0, 6.7)	2.60 (14.0, 7.0, 6.7)	0.85 (t, 7.0)	

^a Refer to the charts in the text. The numbering is based on standard retinoid nomenclature used for the precursor Schiff bases shown in the accompanying tables. Except as noted, values in parentheses are doublet, double doublet, or doublet of doublet of doublet splittings; δ values are not parenthesized and are singlets unless followed by parentheses. ^b Those assignments indicated by an asterisk (*) along any row may be reversed. ^c These refer to the *n*-butylamine side chain. ^d These substances were accompanied by varying amounts of the open-chain Schiff base (obsc, DHP peak obscured by accompanying Schiff base).

by UV-vis spectroscopy and measuring the rate of electrocyclicization by ^1H NMR spectroscopy. The reaction of the retinal **3a** with 1.1 molar equiv of *n*-butylamine at 0 $^\circ\text{C}$ for 10 min led to the replacement of the retinal absorption [abs EtOH, λ_{max} 330 nm (ϵ 18 200), 365 nm (sh, ϵ ~18 000)] by that of the Schiff base [abs EtOH, λ_{max} 331 nm (ϵ 19 000)]. After filtration, removal of solvent on a vacuum pump (~30 min total from the time of mixing *n*-butylamine with retinal **3a**) was followed by dilution of the residue in C_6D_6 . The ^1H NMR spectrum of the sample revealed the presence of a mixture of the expected Schiff base **3b** and DHP-**7b** in an approximately 2:1 ratio. At 23 $^\circ\text{C}$, **3b** rearranged completely to **7b** with $\tau_{1/2}$ ~ 11.4 min (Figure 2). Once formed, the DHP-**7b** could be heated at 78 $^\circ\text{C}$ for at least

14 h without significant change (by ^1H NMR analysis).

By analogy with the mechanistic pathway discussed above for the geometric isomerism of 11,13-dicis to 13-cis aldehydes, the isomeric 11,13-dicis Schiff base **5b** should isomerize to the same DHP-**7b**. This was indeed found to be the case. Freshly purified 13-*tert*-butyl-11,13-dicis-retinal (**5a**) (accompanied by 8% of the 13-cis isomer, **3a**²²) when treated with *n*-butylamine (method A) afforded Schiff base **5b** accompanied by 18% of DHP-**7b**. By

(22) It is generally difficult to obtain pure samples of 11,13-dicis-retinal and its analogues because of their propensity to isomerize to the corresponding 13-cis isomers even at room temperature during their preparation and purification.

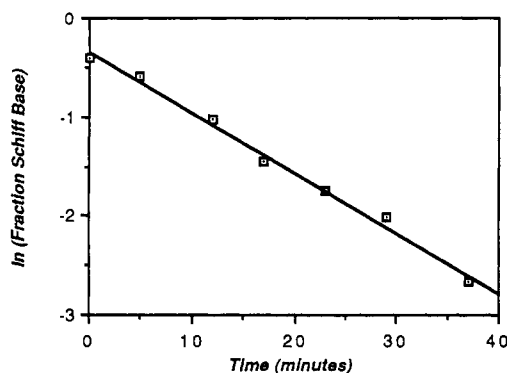


Figure 2. Plot of \ln (fraction **3b**) versus time for the rearrangement of **3b** to **7b**. By monitoring the ^1H NMR signals attributed to the methylene signals of the *n*-butyl group α to the nitrogen of reactant and product (δ 3.50 for the Schiff base **3b**; δ 2.82 plus 2.53 for DHP-**7b**), the half-life for the electrocyclization reaction (assuming an irreversible first-order kinetic rate law) in C_6D_6 at 23°C was determined to be 11.4 ± 0.4 min.

monitoring (^1H NMR analysis) as above, the latter mixture of **5b** and DHP-**7b** in C_6D_6 was demonstrated to afford only the same DHP-**7b** with $\tau_{1/2} \sim 4$ min at 78°C , a process slower than the complementary transformation of **3b** to the same DHP.

Thermal experiments with the *tert*-butylamine-derived Schiff bases of **3a** and **5a**, namely, **3c** and **5c**, respectively, proved particularly informative in that all three species (**3c**, **5c**, and DHP-**7c**) involved in the electrocyclic interconversions could be observed to equilibrate. Treatment of 13-*cis*-**3a** with *tert*-butylamine (method A) afforded a mixture of **3c** (75%), DHP-**7c** (18%), and **5c** (7%) as depicted in Figure 3A at $t = 0$ min (^1H NMR analysis, C_6D_6 at room temperature). Similarly, Figure 3B (at $t = 0$ min) reveals the presence of 10% **3c**, no DHP-**7c**, and 90% **5c** in a parallel experiment starting from 11,13-dicis aldehyde **5a** and *tert*-butylamine. By heating each of the samples at 78°C , the same mixture of the three components (54% **3c**, 27% **7c**, and 19% **5c**) was obtained after 270 min (starting with either the sample enriched in 13-*cis* isomer **3c** or that enriched in 11,13-dicis isomer **5c**). Figure 3 also depicts the ^1H NMR spectra of the two samples after heating for 15 and 95 min. The attainment of this thermal equilibrium further attests to the genesis of the DHP-**7b** and -**7c** as resulting from thermal six-electron electrocyclization from the azatriene moiety present in both **3b** and **3c** and their 11,13-dicis counterparts **5b** and **5c**, respectively.

It next became of some interest to determine whether the same kind of electrocyclic process was characteristic of the parent Schiff bases of 13-*cis*-retinal (**2a**), especially since the M_{412} intermediate of the bacteriorhodopsin photocycle is presently considered to be

an unprotonated lysine Schiff base of this geometric isomer.^{6b,c,5b,i} In addition, since several spectroscopic studies of protonated *n*-butylamine- and *tert*-butylamine-derived Schiff bases of this geometric isomer have been reported, we wondered whether in fact DHP's were formed in earlier studies of 13-*cis*-retinal Schiff bases but had gone undetected.^{11,12} Our studies in this area are described next.

Schiff Bases of the Parent System: *all-trans*-Retinal (1a**) and 13-*cis*-Retinal (**2a**).** The *n*-butyl Schiff bases of *all-trans*-**1a** (method A) and 13-*cis*-**2a** (method A or B) were examined first. Although both **1b** and **2b** are relatively stable at room temperature in the dark for short periods of time, heating (C_6D_6 , 78°C) causes other processes to occur, including geometric isomerism (vide infra). We have invariably found in all our attempts using method A or B to prepare the *n*-butyl Schiff base 13-*cis*-**2b** the formation of variable amounts (5–8%) of the electrocyclized product **9b**. Furthermore, the composition of the mixture obtained upon heating the 13-*cis*-retinal Schiff base **2b** depends on the number of equivalents of amine used. The results obtained upon heating the Schiff bases obtained with 1.1 (Figure 4A) or 5 (Figure 4B) molar equiv of *n*-butylamine by method B reveals an unexpected role played by the excess of *n*-butylamine in inducing the isomerization of the 13-*cis* double bond (**2b**) to the *trans* geometry (**1b**). With 1.1 molar equiv of amine for preparing **2b** (see Figure 4A for the time course), the Δ^{13} isomerization process is small (5% **1b**, 65% **2b**, and 33% DHP-**9b**) after short reaction time (15 min, 78°C), wherein electrocyclization has proceeded to a considerable extent. Figure 5 depicts the ^1H NMR spectrum of the mixture at this particular 15-min time point. The relative amount of DHP-**9b** under these conditions is at a maximum between 15 and 60 min (**2b**:**9b**:**1b** of 60:33:8 was obtained after 30 min). When **2b** is prepared in the same manner starting with a 5-fold molar excess of *n*-butylamine and then the ^1H NMR analysis (see Figure 4B for the time course) carried out after an identical 15-min heating at 78°C , the Δ^{13} isomerization process is substantially greater (25% **1b**, 48% **2b**, and 27% DHP-**9b**), although the relative amount of DHP-**9b** is qualitatively similar (33% in Figure 4A versus 27% in Figure 4B). Comparing panels A and B of Figure 4 reveals that after 10-h heating (78°C) there is a qualitative resemblance of the relative amounts of starting **2b** and isomerization products (a new Schiff base assigned as the 9-*cis* isomer **11b** is also formed more slowly; vide infra). Table I also provides ^1H NMR data for several parent retinal (**1**, **2**, **11**, and **12**) (Chart III) *n*-butylamine- and *tert*-butylamine-derived Schiff base derivatives in C_6D_6 . It must be emphasized that significant amounts of new impurities (^1H NMR analysis) are already apparent after heating for 1 h. Thus, panels A and B of Figure 4 represent only relative amounts of the four components being monitored.

Figure 6 depicts the time course for the thermolysis of the parent

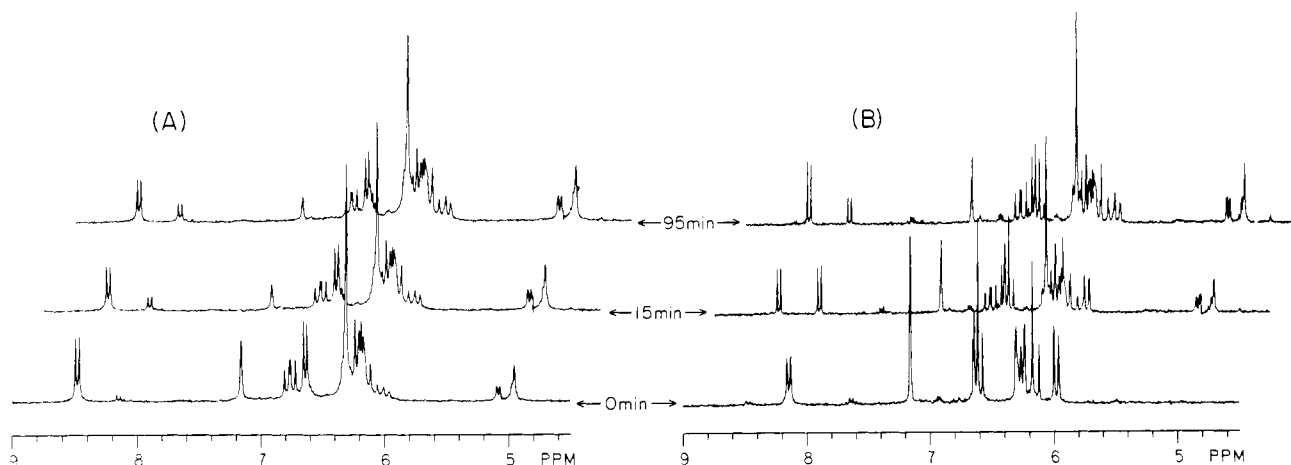


Figure 3. Rearrangement of *tert*-butyl Schiff bases 13-*cis*-**3c** (panel A) and 11,13-dicis-**5c** (panel B) in C_6D_6 at 78°C monitored by ^1H NMR analysis (300 MHz) at $t = 0$, 15, and 95 min. The following ratios were determined by integration of the signals at δ 8.48 (H_{15} of **3c**), 5.07 (H_{11} of **7c**), and 8.14 (H_{15} of **5c**): (panel A) 75/18/7 ($t = 0$); 55/29/16 ($t = 15$); 47/32/21 ($t = 95$). (Panel B) 10/0/90 ($t = 0$); 40/23/37 ($t = 15$); 47/32/21 ($t = 95$). After prolonged heating at 78°C , the ratios of the components were similar although some sample deterioration was evident: 270 min, 54/27/19; 810 min, 51/32/17. Thus, after 95 min to 13.5 h of heating, the ratio **3c**/**7c**/**5c** from heating either **3c** or **5c** remained constant ($\sim 5/3/2$).

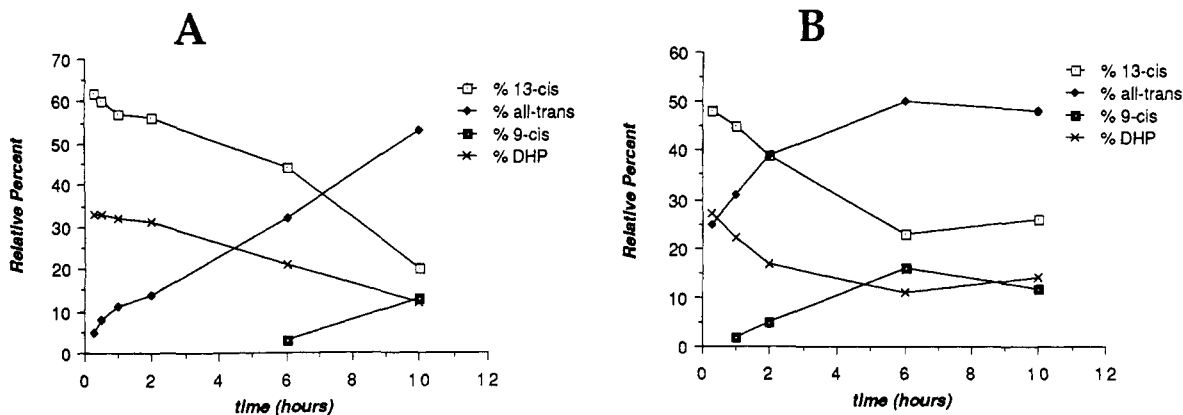


Figure 4. Time course for the thermolysis (C_6D_6 , $78^\circ C$) of the *n*-butylamine Schiff base **2b** of the parent 13-*cis*-retinal (**2a**). The samples were prepared by method B using 1.1 molar equiv (graph A) and a 5 fold molar excess (graph B) of *n*-butylamine. Relative percentages of the four components indicated were followed over a 10-h period. After 10 h, the relative ratios of **2b**/**1b**/**11b**/**9b** were as follows: (A) 22/53/13/12; (B) 26/48/12/14. Within the first hour, the production of unidentified minor components as evidenced by a myriad of base-line 1H NMR signals became apparent. Therefore, the data represent only relative yields. Figure 5 gives the 1H NMR spectrum of a typical sample of **2b** after brief heating. See Tables I and II for 1H NMR data in C_6D_6 or $CDCl_3$ for Schiff base derivatives of various parent retinals.

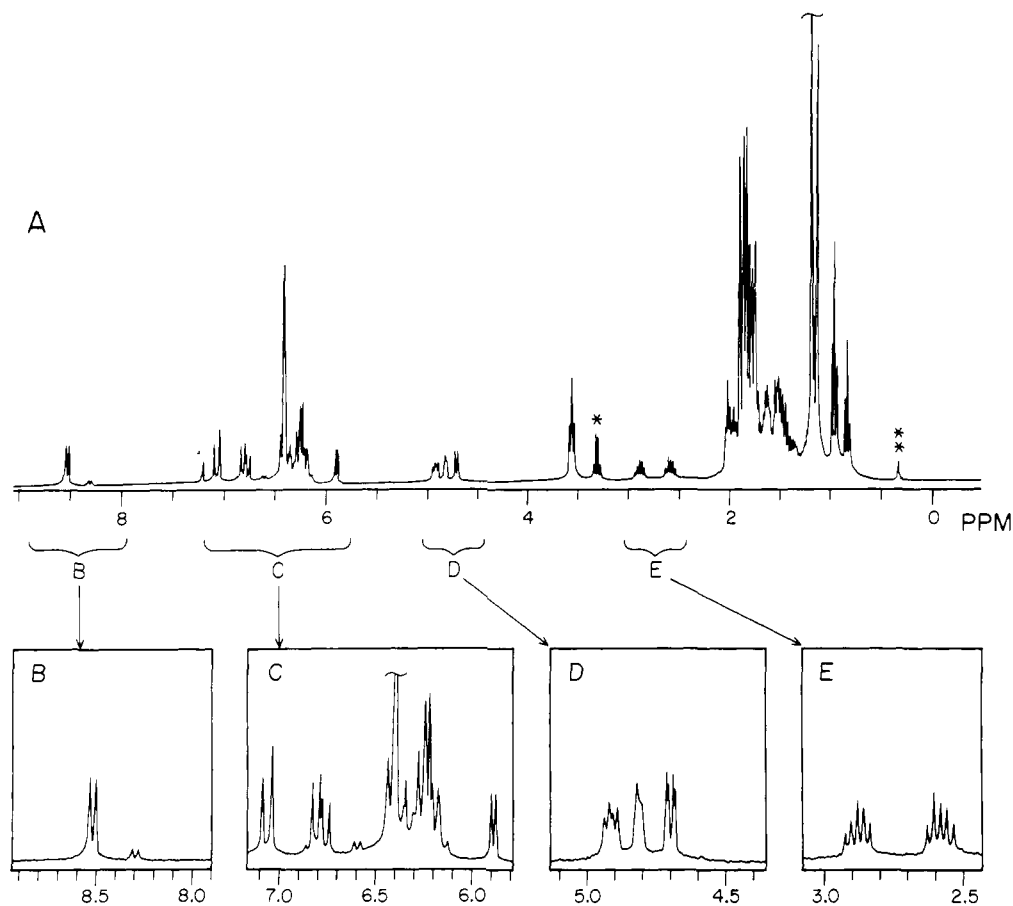


Figure 5. 1H NMR spectrum (300 MHz, residual protio C_6D_6 signal at δ 7.16) of *n*-butylamine (1.1 molar equiv using method B) derived Schiff base **2b** in C_6D_6 after 15 min of heating at $78^\circ C$ [(*) residual ether; (**) impurity signal at δ 0.41 present in C_6D_6]. Panels B–E are expansions of the regions indicated in panel A. Panel B shows the H_{15} doublets assigned to **2b** (δ 8.52) and **1b** (δ 8.25). The high-field doublet (δ 5.89) in panel C and the signals shown in panels D and E are assigned to DHP-**9b**. See Figure 4 and Tables I and III for additional details.

all-trans-retinal *n*-butylamine Schiff base (**1b**), and it is clear that the major isomers present after prolonged heating include (relative amounts) starting **1b** (57%), 13-*cis*-**2b** (27%), and 9-*cis*-**11b** (16%). However, as indicated in the caption to Figure 6, small amounts of DHP-**9b** could be detected along with other unknown constituents. It is informative to note that from the results shown in Figure 4 the relative amounts of **1b**/**2b**/**11b** were 58%/28%/16% (average of the two experiments summarized in Figure 4 excluding the presence of DHP-**9b**). Thus, the relative amounts of the three parent Schiff bases presented in Figures 4 (starting from 13-*cis*-**2b**) and 6 (starting from the corresponding *all*-

trans-**1b**) taken collectively are in good agreement and probably represent an equilibrium ratio of products. There is no question however that deterioration of sample becomes increasingly significant on prolonged heating of either **1b** or **2b**. Sample deterioration is less of a problem for *tert*-butylamine-derived Schiff bases of *all-trans*-**1a** and 13-*cis*-**2a** (i.e., **1c** and **2c**), which are discussed next.

The presence of the *tert*-butyl group made monitoring the isomerization reaction simpler by rendering negligible the electrocyclic process. This is apparently due to the presence of the bulky *tert*-butyl group on the nitrogen, one end of the reacting

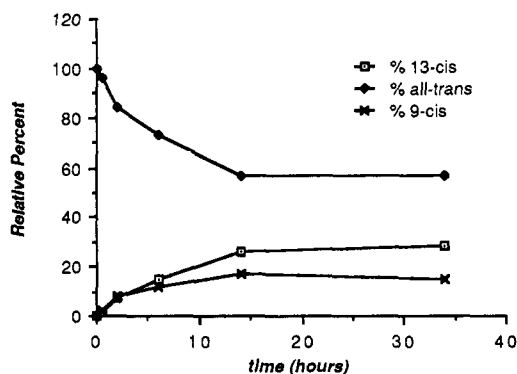
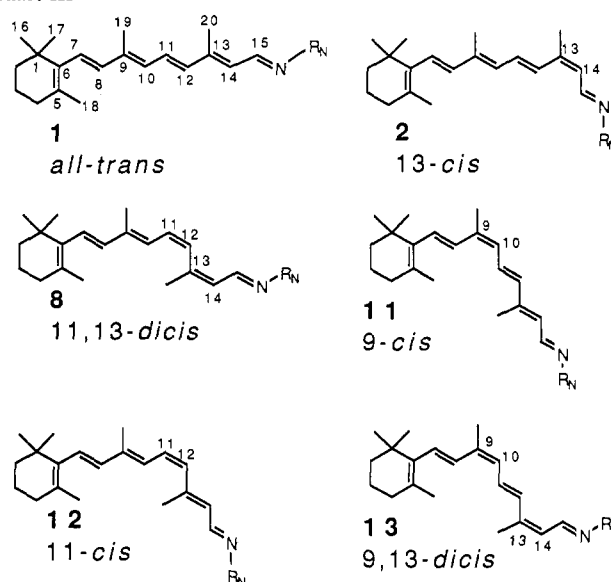


Figure 6. Time course for the thermolysis (C_6D_6 , 78 °C) of the *n*-butylamine Schiff base **1b** of the parent *all-trans*-retinal (**1a**). At the initial time point (room temperature), the 1H NMR spectrum (C_6D_6) was quite clean; most notably, extraneous peaks were not detected in the region δ 5–11. After 30 min of heating at 78 °C, the relative composition as estimated by 1H NMR analysis was 2% 13-*cis*-, 3% 9-*cis*-, and 96% starting *all-trans*-retinal. However, after 2 h of heating (8% 13-*cis*-, 9% 9-*cis*-, and 84% *all-trans*-retinal) signals in the region near δ 2.5 and 4.5–5.0 (indicative of the presence of DHP-**9b**) were clearly discernible. At longer reaction times (14–34 h), the relative amounts of the three major isomers remained relatively constant (27% 13-*cis*-, 16% 9-*cis*-, and 57% *all-trans*), but there appeared an extensive and complex array of weaker signals in the region δ 3.4–7.

termini involved in cyclization.^{14c,d} The *tert*-butylamine-derived Schiff bases *all-trans*-**1c** and 13-*cis*-**2c** were prepared with method A and submitted to the usual thermal conditions (C_6D_6 , 78 °C; 1H NMR analysis). Figure 7 summarizes the results in a side by side comparison of the time course for the rearrangement of the *all-trans* (Figure 7A) and 13-*cis* (Figure 7B) isomers. As can be seen in Figure 7A, heating Schiff base **1c** led to slow geometric isomerism at similar rates to those of the more substituted Δ^{13} and Δ^9 double bonds to give 13-*cis*-**2c** and 9-*cis*-**11c** isomers (and a small amount of what has been tentatively assigned as the doubly isomerized 9,13-dicis isomer **13c**, which starts appearing after ~6 h). Results obtained for heating **2c** (Figure 7B) nicely complement the results from the preceding experiment (Figure 7A). The relative proportions of **2c**/**1c**/**11c**/**13c** after prolonged heating (~15 to >32 h) were estimated to be 19%/56%/20%/6%, an apparent equilibrium ratio of products. These results are not too dissimilar to the results obtained for heating the corresponding *n*-butyl Schiff bases (Figures 4 and 6). However, there was no indication of the formation of DHP-**9c**, and the 1H NMR spectra were considerably cleaner than those from the *n*-butyl Schiff base experiments.

In view of the formation of yet new Schiff base isomers possessing 9-*cis* or 9,13-dicis geometry in the thermolysis of 13-*cis*

Chart III



a, $N-R_N = O$; b, $R_N = n\text{-Bu}$; c, $R_N = \text{tert-Bu}$

(Figures 4, 5, and 7) and *all-trans* isomers (Figure 6 and 7), it became of interest to examine the behavior of Schiff bases of 9-*cis*-retinal (**11a**). Figure 8 depicts the time course for the thermolysis of the *n*-butyl (**11b**) and *tert*-butyl Schiff bases (**11c**) possessing 9-*cis* geometry, and it is apparent that on prolonged heating the same set of four isomers (*all-trans*-**1**, 9-*cis*-**11**, 13-*cis*-**2**, and 9,13-dicis-**13**) are involved. Again, *all-trans*-**1** begins appearing as the major component on prolonged heating. Although the thermolysis of the *n*-butyl Schiff base **11b** (Figure 8A) was characterized by production of a myriad of new minor components, as was the case for the corresponding *n*-butyl Schiff bases **2b** (Figure 4) and **1b** (Figure 6), the *tert*-butyl Schiff bases **11c** (Figure 8B), **2c** (Figure 7B), and **1c** (Figure 7A) afforded cleaner and, at least qualitatively, mutually consistent results. Namely, in all cases an equilibrium was approached consisting of ~50–60% of *all-trans*-**1c**, comparable amounts (~20%) of 13-*cis*-**2c** and 9-*cis*-**11c**, and minor amounts (~6–12%) of 9,13-dicis-**13c**. As in the case of **1c** and **2c** there was no indication that prolonged heating of **11c** (~60 h at 78 °C) afforded any DHP-**9c** (which could have resulted from **2c** or **13c**) as indicated by examination of the δ 5.0 region in the 1H NMR spectra of the thermolysis mixture. Throughout all of the thermal rearrangement studies of the parent retinal Schiff bases, the possible production of Schiff

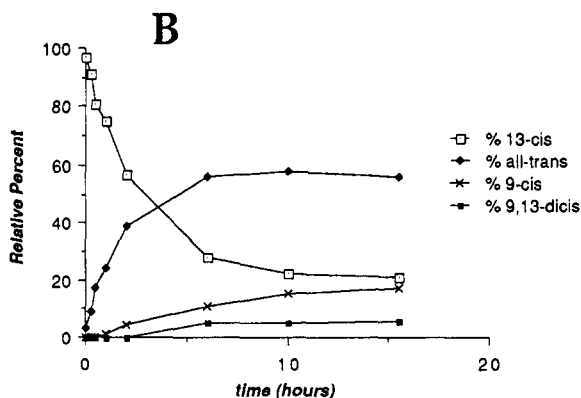
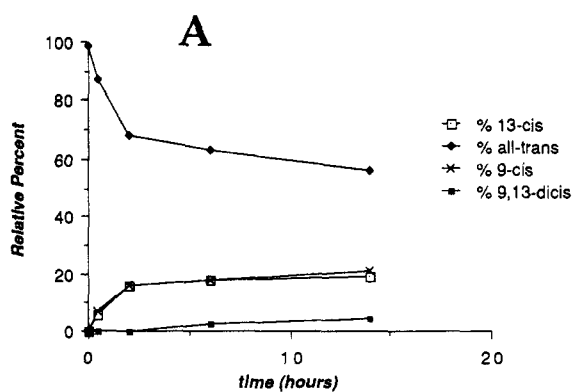


Figure 7. Time course for the thermolysis (C_6D_6 , 78 °C) of the *tert*-butylamine Schiff bases **1c** (graph A) and **2c** (graph B) of the parent *all-trans*-retinal (**1a**) and 13-*cis*-retinal (**2a**) (both prepared by method A). Analysis by 1H NMR spectroscopy indicated for both samples that even after prolonged heating (>14 h) the base line in the region δ 2.0–5.5 of their spectra remained relatively free of extraneous signals (in contrast to the experiments with *n*-butyl Schiff bases shown in Figures 4 and 6). 1H NMR analysis of the sample of **1c** revealed it to be free of geometric isomers; that of **2c** was initially contaminated by ~3% of **1c** resulting from aldehyde **1a** already present in the starting **2a**. After prolonged heating (14 to >32 h), the relative amounts of geometric isomers from heating **1c** to **2c** remained relatively constant: 19 \pm 2% 13-*cis*; 56 \pm 2% *all-trans*; 20 \pm 3% 9-*cis*; and 6 \pm 2%, 9,13-dicis. The identity of the minor 9,13-dicis isomer must be regarded as tentative since an authentic specimen was unavailable.

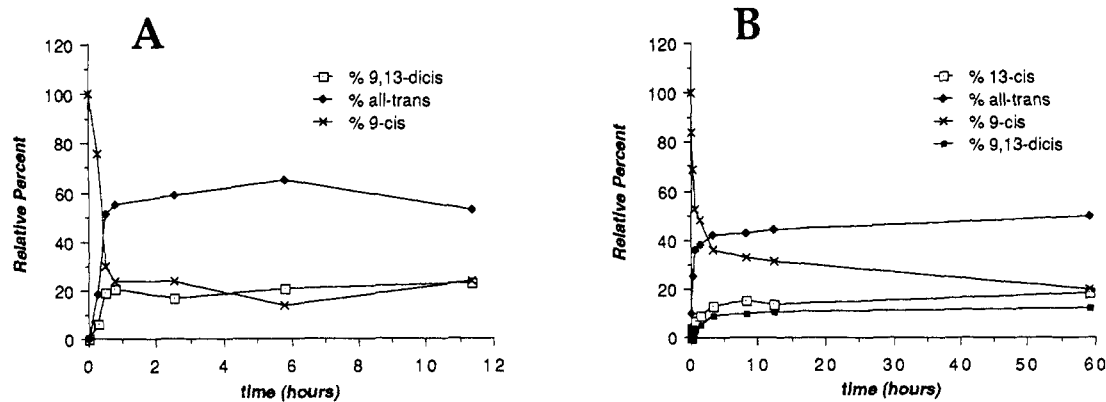


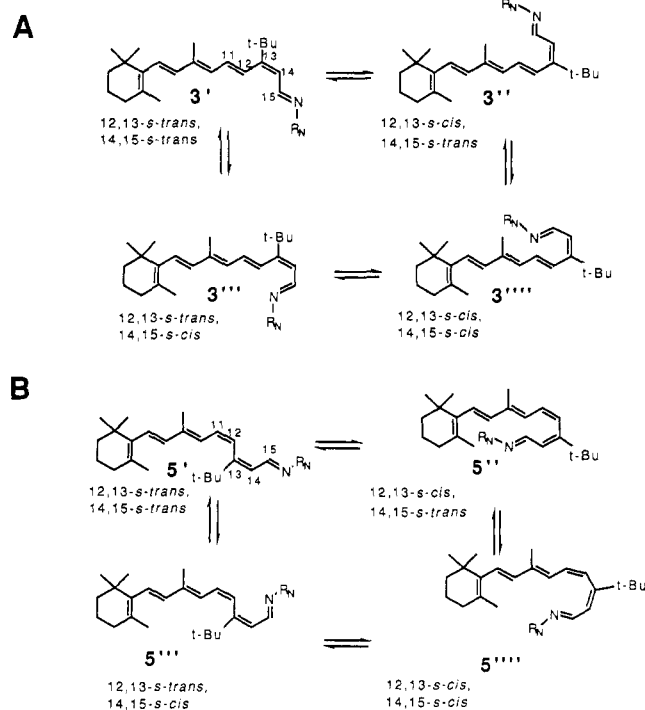
Figure 8. Time course for the thermolysis in C_6D_6 at $78^\circ C$ of the *n*-butyl (**11b**) (graph A) and *tert*-butyl Schiff base (**11c**) (graph B) of the parent 9-*cis*-retinal (**11a**). The substrate indicated as the 9,13-dicis isomer may be admixed with the 13-*cis* isomer **2b** in graph A, but this could not be confirmed. Note that only relative percentages are given, that the thermal experiment of graph A leads to a myriad of minor peaks in the δ 3–5.5 region of the 1H NMR spectrum, and that the experiment described in graph B was much less complex. The latter reaction could be carried out to quite long reaction times (i.e., 60 h) without the appearance of complex base-line peaks in the δ 3–5.5 region. See Experimental Section for additional details.

base **12b** or **12c** of parent 11-*cis*-retinal (**12a**) was also monitored (see Table I for 1H NMR data of independently synthesized samples). There was never any indication that the expected thermodynamically less stable 11-*cis* isomer was produced.

Having now presented the results obtained for the 13-*tert*-butyl analogues and the parent system, it is useful to digress here on the matter of the factors affecting thermodynamic preferences of DHP versus the open-chain polyene Schiff base. Whereas the ternary equilibrium between **5a**, **7a**, and **3a** is such that the oxa heterocycle **7a** (α -dihydropyran) cannot be detected by examination of the 1H NMR spectrum, that between **5b**, **7b**, and **3b** favors aza heterocycle **7b** (1,2-dihydropyridine) exclusively. It can be conjectured that due to the shorter O–C bond length relative to the N–C bond length there may exist greater ring strain in the oxa heterocycle than in the nitrogen system. Moreover, from the relative electronegativities of oxygen versus nitrogen, resonance stabilization in the former (a dienol ether) should be smaller than that in the latter (a dienamine) in terms of heteroatom lone pair delocalization. Either factor should render the aza heterocycle more likely to dominate than the oxa heterocycle with respect to their open-chain counterparts (Schiff base and aldehyde, respectively). However, it is hardly clear from a quantitative standpoint where the equilibrium should lie as exemplified by the finding that **3b** and **5b** on heating prefer to exist completely as **7b** whereas **3c**, **5c**, and **7c** coexist at equilibrium. A subtle balance of steric factors seems to be playing a role, but these are hardly well-defined at this time.

It is convenient now to also digress on the matter of a comparison of the thermal results obtained for the 13-*cis* geometric isomer of 13-*tert*-butyl Schiff bases (derived from aldehyde **3a**) and those for the parent system (derived from **2a**) just discussed. For **3**, consider the four rotamers (considering only the *s*-cisoid or *s*-transoid arrangements about the Δ^{12} and Δ^{14} single bonds) **3'**–**3''''** (Scheme 1A). We^{13b} and others^{10b} have reported that 13-*tert*-butyl-13-*cis*-retinal (**3a**) exists predominantly in the 12,13-*s*-*cis* conformation (probably a twisted **3a''** rather than **3a''''**). Of course the conformer **3''''** is required for six-electron electrocyclization, and it is our contention that because the Schiff bases **3b** and **3c** exist mainly in the 12,13-*s*-*cis* conformation **3'**, it need only undergo 14,15-*s*-*trans* to 14,15-*s*-*cis* rotation prior to electrocyclization. In contrast, the parent 13-*cis* isomer **2** is predominantly in the *s*-*trans*,*s*-*trans* conformation corresponding to **3'** (*tert*-butyl replaced by a methyl), and both single bonds must rotate to *s*-*cis*,*s*-*cis* in order to electrocyclize. This reordering of rotamers is one factor that raises the relative activation energy for electrocyclization in the parent system **2**; perhaps to state this more correctly, less rotational reordering is required of **3** to assume the proper conformation **3''''** for facile electrocyclization. Thus, a simple entropic argument in part serves to rationalize how introduction of a bulky group at C_{13} (**3**) facilitates the thermal electrocyclization of **3** relative to **2**. Another significant feature

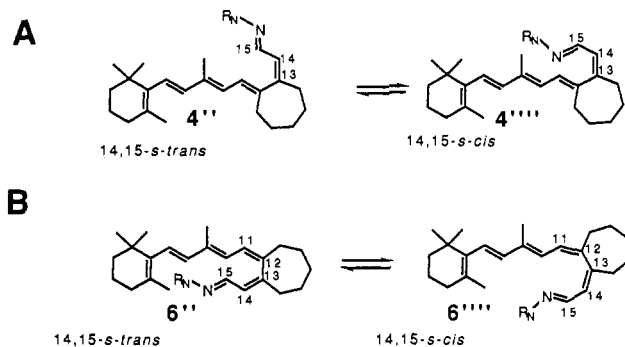
Scheme I



of the 13-*tert*-butyl-substituted system **3** is that the Δ^{13} geometry is locked (or at least strongly biased) in the *cis* geometric configuration due to the presence of the bulky *tert*-butyl group. This feature likely simplifies the thermal behavior of **3** relative to **2** by attenuating Δ^{13} isomerization.

It is not altogether clear how the Schiff bases derivatives of **2** undergo *cis*–*trans* geometric isomerism along the polyene chain, but one can envisage pathways involving a direct π -bond rotation, deprotonation–rotation–reprotonation via an enamine intermediate, or a Michael addition–rotation–retro-Michael process via other enamine intermediates. There is certainly some indication that excess amine may play a role in the isomerization process (see Figure 4), but to be sure, a clear rationale has not emerged. Of course upon heating the Schiff bases of *tert*-butyl-substituted system **3**, geometric isomerism about the Δ^{13} or Δ^9 double bonds is minimal compared to the situation for **2**. Any of the possible modes of geometric isomerism just mentioned would probably be attenuated by the presence of the bulky *tert*-butyl group at C_{13} . As was seen earlier in several cases, a *tert*-butyl group on nitrogen also strongly influences the thermal processes. The *tert*-butyl Schiff base **3c** electrocyclizes more slowly (heating at $78^\circ C$ is required) than the corresponding *n*-butyl Schiff base **3b** ($\tau_{1/2} \sim$

Scheme II



11 min at 23 °C), and *n*-butyl Schiff base **2b** electrocyclizes to a significant degree whereas *tert*-butyl Schiff base **2c** does not. These two examples merely reflect the finding that introduction of bulky groups at the termini of polyenes undergoing electrocyclic ring closure generally attenuates the rate of electrocyclic ring closure.^{14c,d} A similar steric retardation of rate is seen in the cyclization of the 11,13-dicis isomer of **3b**. Namely, the *n*-butyl Schiff base **5b** cyclizes to the same DHP (**7b**) as **3b**, but with $\tau_{1/2} \sim 4$ min at 78 °C. One can readily see by examining the four rotamers **5'-5'''** (Scheme 1B) corresponding to **3'-3'''** (Scheme 1A) that the requisite **3'''** needed for cyclization to **7** should be sterically more accessible than **5'''** needed for cyclization to the identical **7**.

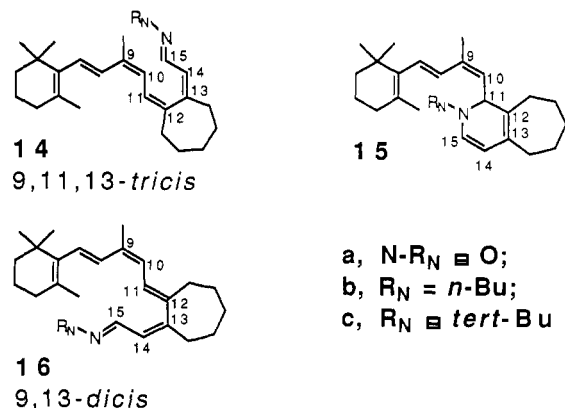
Schiff Bases of 12,20-Tetramethylenetetrals. As just discussed the facility of the electrocyclization of **3b** and **5b** to **7b** is attributed to the finding that these structures probably exist predominantly in the 12,13-*s-cis* conformations **3b''** and **5b''** (as shown by NOE studies^{10b,13b} of the retinals **3a** and **5a**), requiring only the rotation of their 14,15-*s*-bond from the *trans* to the *cis* conformation in order to fulfill the topographical requirement for the cyclization. We have been working for some time with 12-*s-cis*-locked retinoids as models for the study of the effect of rotationally restricted structures on the chemical and spectroscopic properties of these polyenes.^{13d,f-h} We have described the synthesis and spectral properties of the eight 7-*trans* isomers of the 12,20-tetramethylenetetrals, and accordingly, we extended the present study to the corresponding Schiff bases of **4a** and **6a** and several other isomers.

As anticipated, the behavior of the Schiff bases with 13-*cis* geometry and 12-*s-cis*-locked conformation is similar to that described for the 13-*tert*-butyl analogues, although the thermal cyclizations take place at a somewhat slower rate. Treatment of 13-*cis* isomer **4a** with *n*-butylamine led to the observation of an ca. 1:1 mixture of the Schiff base **4b** and DHP-**10b**, which upon standing at room temperature (23 °C) was completely transformed to **10b** with a half-life of ~ 70 min. On the other hand, the 11,13-dicis aldehyde **6a** afforded only the Schiff base **6b** upon treatment with *n*-butylamine under the same conditions. The latter **6b** was converted into the same DHP-**10b** with a half life of ~ 10 min under more forcing conditions (C_6D_6 , 78 °C). The greater stability of the *tert*-butyl Schiff bases **4c** and **6c** was evident from the formation of these Schiff bases uncontaminated by **10c** from the reaction of the retinals **4a** and **6a**, respectively, with *tert*-butylamine in the usual manner (method A).

As shown in Scheme II, the Schiff bases of **4a** and **6a** are conformationally restricted to the 12-*s-cis* conformation. Other than the possibility that seven-membered ring fusion might be preventing optimal orientation of the azatriene unit undergoing electrocyclic ring closure, it is not easy to see why **4b** and **6b** should cyclize more slowly to **10b** compared to the cyclization of **3b** and **5b** to **7b**. In point of fact, some of our earlier results in the vitamin D field suggest seven-membered ring fusion might actually facilitate electrocyclic ring closure.²³

Finally, since 9,11,13-tricis aldehyde **14a** (Chart IV) was also readily available from previous studies^{13h} in this laboratory, its

Chart IV



n-butylamine Schiff base **14b** was also prepared, and it cyclized on brief heating (30 min, 78 °C) completely to the 9-*cis*-DHP **15b**. The less hindered *n*-butyl Schiff base 9,13-*dicis*-**16b** was transformed to the same 9-*cis*-DHP **15b** even at room temperature. Thus, at least qualitatively, the thermal behavior of 9,11,13-*tricis*-**14b** resembles that of 11,13-*tricis*-**6b**, and the behavior of 9,13-*dicis*-**16b** resembles that of 13-*cis*-**4b**. In other words, the presence of the Δ^{11} -*cis* double bond attenuates the rate of electrocyclic ring closure through what was discussed earlier as a steric effect. The presence of a 9-*cis* double bond as in **14b** and **16b** at least qualitatively did not seem to significantly influence their cyclization to **15b**.

Additional Studies. At least one aspect of the chemical reactivity of the DHP-**7b** has already been discussed. In contrast to the ring closure and ring opening considered to be responsible for the equilibration between *N-tert*-butyl systems **3c**, **7c**, and **5c**, the *n*-butyl DHP-**7b** was found to be thermally stable, being recovered essentially unaltered after 14 h at 78 °C. With the availability of **7b**, the question arose whether protonation of **7b** on nitrogen might induce ring opening through the intermediacy of **17** (Scheme III). It was reasoned that ene-ammonium salt **17**²⁴ might undergo facile electrocyclic ring opening to **18**, the driving force being the ability of the latter to delocalize the positive charge on nitrogen. In the event, treatment of a ¹H NMR pure sample of **7b** in CD_2Cl_2 with excess trifluoroacetic acid afforded what has been assigned as the 2,3-dihydropyridinium salt **19**.^{25,26} At least for DHP-**7b**, a kinetically competent process for inducing its ring opening to **3b** or **18** has not been successfully realized.

Summary

We have thus found that 12-*s-cis*-biased 13-*cis*-retinals form Schiff bases²⁷ that are prone to electrocyclize to 1,2-dihydropyridines (DHP's). The factors affecting the rate of cyclization are at least partially understood on the basis of steric and conformational effects.²⁸ Factors affecting thermodynamic preferences (DHP versus the open polyene Schiff base form) have not yet been fully evaluated. Studies of simpler, more stable systems are under way. Some caution needs to be taken in the use of 13-*cis*-retinal Schiff bases as spectroscopic models to ensure identity of the Schiff bases. Finally, initial studies indicate that

(24) The simple *N,N*-dimethyl-1,2-dihydropyridinium salt has been synthesized. See Saunders, M.; Gold, E. H. *J. Am. Chem. Soc.* **1966**, *88*, 3376.

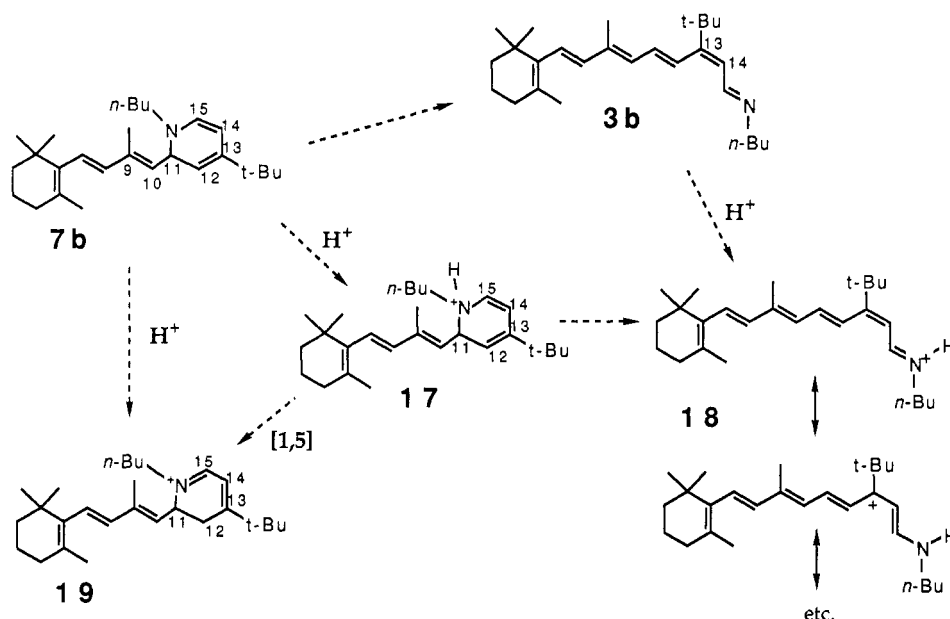
(25) For a theoretical study of the formation, stability, and protonation of dihydropyridines, see Bodor, N.; Pearlman, R. *J. Am. Chem. Soc.* **1978**, *100*, 4946.

(26) Treatment of **7b** with oxidizing agents including dimethyl disulfide, chloranil, or tris(4-bromophenyl)aminium hexachloroantimonate appears to induce oxidation of the dihydropyridine to the pyridinium salt as reflected by the appearance of low-field ¹H NMR peaks. However, the ¹H NMR spectra obtained were quite complex (consisting of numerous minor peaks).

(27) It has been suggested that the chromophore in bR^A exists in the 12-*s-cis* conformation. Besides ref 111, see also: (a) Muradin-Szweykowska, M.; Broek, A. D.; Lugtenburg, J.; van der Bend, R. L.; van Dijk, P. W. M. *Rec. Trav. Chim. Pays-Bas* **1983**, *102*, 42. (b) Muradin-Szweykowska, M.; Peters, A. J. M.; Lugtenburg, J. *Rec. Trav. Chim. Pays-Bas* **1984**, *103*, 105.

(28) Besides the ring size effects cited in ref 23, alkyl group effects on the rate of electrocyclizations of hexa-1,3,5-trienes have been reported. See: Spangler, C. W.; Jondahl, T. P.; Spangler, B. *J. Org. Chem.* **1973**, *38*, 2478.

Scheme III



protonation (or oxidation²⁶) does not lead to ring-opened products. The significance, if any, of the formation of DHP's or the occurrence of other pericyclic processes to the photocycle of bacteriorhodopsin or other retinal-containing pigments is an intriguing question.²⁹ In any event, studies of the thermal isomerization of Schiff bases of model systems should continue to serve as useful reference points for understanding *in vivo* isomerization pathways.

Experimental Section

General Spectroscopic Data. The ^1H nuclear magnetic resonance spectra (^1H NMR) were obtained on a 300-MHz GE QE-300 or a Nicolet NT-300 spectrometer with benzene- d_6 (C_6D_6), dichloromethane- d_2 (CD_2Cl_2), or chloroform- d_1 (CDCl_3) as solvent (the residual protio peak of the solvent served as the internal standard: C_6D_6 , δ 7.16; CD_2Cl_2 , δ 5.33; CDCl_3 , δ 7.26). The chemical shifts are given in δ values and the coupling constants (J) in hertz (Hz). The ^{13}C nuclear magnetic resonance (^{13}C NMR) spectra were obtained on a 75.5-MHz GE QE-300 or a Nicolet NT-300 spectrometer with CDCl_3 as solvent and internal standard. Chemical shifts are given in δ values. Infrared spectra were obtained on a Perkin-Elmer Model 283 grating spectrophotometer using 0.1-mm NaCl plates with the solvent as indicated. Ultraviolet spectra were obtained on a HP 8451A diode array UV-vis spectrophotometer with the appropriate solvent.

All experiments involving air- and/or moisture-sensitive materials were carried out under an inert atmosphere of argon or nitrogen, which was dried prior to use by passage through a column of KOH layered with CaSO₄. Solvents and other chemicals used for preparative work were of reagent grade and dried as necessary according to standard procedures. The aldehydes were prepared by previously described¹³ methods or obtained commercially and were purified as necessary by high-pressure liquid chromatography (HPLC). The latter was performed with a Waters 6000A or 510 pump and a R401 refractive index detector. Flash chromatography was performed on silica gel (Sigma, 230–400 mesh).

Preparation of Schiff Bases. All reactions were carried out under an inert atmosphere and in a dark room equipped with dim red lights.

(A) Method A. To a cooled (0 °C) solution of the retinal (~30 mg) in anhydrous EtOH (2 mL) containing 4A molecular sieves was added under nitrogen a 5-fold excess of the amine. Stirring was continued for 1 h at 0 °C, and then the molecular sieves were removed by filtration followed by washing the solid repeatedly with anhydrous ethyl ether. The filtrate containing solvent and amine was evaporated to dryness (rotary evaporator and oil pump) to give a residue which was used directly as obtained. The residue was dissolved in dry ether to afford a standard stock solution (molarity based on an assumed quantitative yield of Schiff base), aliquots of which were transferred to separate vessels according to the amount needed. The ether was again removed under vacuum from individual aliquots, and then each residue was diluted with the appropriate solvent as desired. For example, for ¹H NMR spectra, an appropriate quantity of C₆D₆ was added, and then the solution was trans-

ferred to an amber (protection against light) NMR tube. Additional protection against light was achieved by covering the NMR tube with aluminum foil whenever feasible.

(B) Method B. For the more reactive retinals and amines, it was possible to utilize near-equimolar amounts of these substrates for Schiff base production at 0 °C. With a procedure similar to that described above, parent 13-*cis*-retinal (**2a**) was reacted with 1.1 molar equiv of *n*-butylamine. Monitoring by UV indicated that Schiff base formation was complete within 10 min at ice bath temperature. After removal of the molecular sieves by filtration, the reaction solution was evacuated to dryness (<20 min) on an oil pump, the residue was dissolved in an appropriate solvent (e.g., C₆D₆, CDCl₃, CD₂Cl₂, MeOH, etc.), and then the spectrum (e.g., ¹H NMR or UV-vis spectrum etc.) was recorded. This procedure was utilized successfully in terms of complete transformation to Schiff base with *n*-butylamine, but not *tert*-butylamine, as base. The *n*-butyl Schiff base of 13-*cis*-13-*tert*-butylretinal (**3a**), but not that of parent *all-trans*-retinal (**1a**) or the parent 9-*cis* isomer (**11a**), could also be prepared successfully in this manner. Method B was not examined further for the preparation of any of the other retinal Schiff bases described in this article. This procedure could be useful in certain instances involving unstable Schiff bases and only if the amine and aldehyde are sufficiently reactive toward one another.

Schiff Bases of 13-*tert*-Butyl-13-*cis*-retinal (3a). (A) 1,2-Dihydropyridine **7b**. *n*-Butylamine-derived Schiff base **3b** prepared by method A (1 h at 0 °C and then 1 h at room temperature) exhibited the typical ¹H NMR spectrum attributable to the 1,2-dihydropyridine **7b** as shown in Figure 1 (C₆D₆). As indicated in the caption to Figure 1, the spectrum remains essentially unchanged after prolonged heating (14 h, 78 °C). The ¹H NMR spectral parameters are summarized in Table III for C₆D₆ or CDCl₃ as solvent. Other spectral data were as follows: ¹³C NMR (75.5 MHz, multiplicity given in parentheses—s, d, t, q) δ (CDCl₃) 12.3 (q), 13.9 (q), 19.3 (t), 20.2 (t), 21.7 (q), 29.0 (two q), 30.6 (t), 33.0 (t), 33.5 (s), 34.2 (s), 39.6 (t), 52.3 (t), 55.0 (d), 93.1 (d), 105.8 (d), 126.2 (d), 128.8 (s), 130.3 (d), 131.9 (s), 136.9 (d), 137.5 (s), 137.6 (d), 144.0 (s); UV (ethanol) λ_{max} 266 nm (ε 16 700); UV (hexanes) λ_{max} 264 nm (ε 15 400); IR (CH₂Cl₂) ν_{max} 3020 (w), 2960 (s), 2920 (s), 2860 (s), 1635 (m), 1560 (m), 1460 (m), 1360 (m), 1200 (m), 1180 (m), 1080 (m), 970 (ms) cm⁻¹.

(B) *n*-Butyl Schiff Base 3b. By use of method B (~30 min at 0 °C to less than room temperature; 1:1 molar equiv of *n*-butylamine to 1.0 equiv of **3a**) for sample preparation, the ¹H NMR spectrum in C₆D₆ of a sample of **3b** contaminated by ~33% **7b** could be obtained (data for **3b** summarized in Table I). Monitoring of the absorption spectrum of **3a** and **3b** (see text for discussion) indicated that Schiff base formation was complete within 10 min of mixing **3a** and *n*-butylamine under these conditions. The UV-vis data for **3a** described in the text are more accurate in terms of extinction coefficients than the data previously reported.^{13b} The rate of isomerization of **3b** at 23 °C to DHP-**7b** could be followed as indicated in Figure 2.

(C) *tert*-Butyl Schiff Base 3c and DHP-7c. The *tert*-butylamine Schiff base 3c was prepared by reacting 3a with a 5-fold excess of *tert*-butylamine according to method A. As noted above, method B leads

to incomplete conversion of aldehyde to Schiff base. The ^1H NMR sample consisted of 13-*cis*-**3c**, DHP-**7c**, and 11,13-*dicis*-**5c** in the relative amounts 75%, 18%, and 7%, respectively (panel A in Figure 3). Thermal equilibration of these three components at 78 °C in C_6D_6 led to a 54%, 27%, and 19% distribution of products.

Schiff Bases of 13-*tert*-Butyl-11,13-*dicis*-retinal (5a). (A) *n*-Butyl Schiff Base **5b** and 1,2-Dihydropyridine **7b**. With method A, **5b** was prepared from **5a** and the ^1H NMR spectrum in C_6D_6 of the sample was recorded (see the data in Table I). By a rate study analogous to that described in Figure 2 for the cyclization of 13-*cis*-**3b** to DHP-**7b**, **5b** rearranged to the same DHP-**7b** with $\tau_{1/2} \sim 4.2 \pm 0.2$ min at 78 °C in C_6D_6 .

(B) *tert*-Butyl Schiff Base **5c** and DHP-**7c**. The *tert*-butylamine Schiff base **5c** was prepared by reacting **5a** with a 5-fold excess of *tert*-butylamine according to method A. As noted above, method B leads to incomplete conversion of aldehyde to Schiff base. The starting 11,13-*dicis* aldehyde **5a** was invariably contaminated by small amounts of 13-*cis* aldehyde **3a**.²² Immediately after its preparation, ^1H NMR analysis revealed that the sample consisted of 13-*cis*-**3c** and 11,13-*dicis*-**5c** in 10% and 90% relative yields, respectively (panel B in Figure 3 at $t = 0$ min). No DHP-**7c** was detected initially in contrast to the preparation of **3c**, although heating **5c** afforded the same proportions (54%, 27%, and 19%, respectively) of **3c**, **7c**, and **5c** as obtained for the equilibration experiment starting from **3c**.

Schiff Bases of Parent 13-*cis*-Retinal (2a). (A) *n*-Butyl Schiff Base **2b** and 1,2-Dihydropyridine **9b**. The Schiff base **2b** was prepared by reacting **2a** according to Method B with a 1.1 or 5 molar equiv excess of *n*-butylamine (method A was also used). The ^1H NMR data for **2b** and **9b** and the various thermal experiments are summarized in the text, in Tables I–III, and in Figures 4 and 5.

(B) *tert*-Butyl Schiff Base **2c**. Method A was used to prepare **2c**, and the results are summarized in Tables I and II and in Figure 7B. As indicated by the latter figure, no DHP-**9c** was formed upon heating the sample of **2c** at 78 °C (C_6D_6). Only geometric isomerism was detected (Figure 7B).

Schiff Bases of Parent *all-trans*-Retinal (1a). (A) *n*-Butyl Schiff Base **1b**. The Schiff base **1b** was prepared according to method A (method B failed to give complete conversion of aldehyde to Schiff base) and the results are discussed in the text with additional data in Tables I and II and in Figure 6.

(B) *tert*-Butyl Schiff Base **1c**. The Schiff base **1c** was prepared according to method A, and the results are presented in Tables I and II and in Figure 7A. The results complemented those obtained by heating 13-*cis*-**2c** as shown in Figure 7B in a side by side comparison.

Schiff Bases of 12,20-Tetramethylene-13-*cis*-retinal (4a). (A) *n*-Butyl Schiff Base **4b** and DHP-**10b**. The Schiff base **4b** was prepared from *n*-butylamine and 13-*cis* aldehyde **4a** according to method A. The initial ^1H NMR spectrum recorded revealed the presence of a ~1:1 mixture of **4b** and cyclized product DHP-**10b** (determined by integration of the pair of doublets at δ 4.69 and 4.77 (2 H, assigned to H_{14} and H_{11} of **10b**, respectively) relative to the triplet at δ 3.52 (2 H, assigned to the methylene group α to nitrogen of **4b**)). The rate of cyclization of **4b** to **10b** was followed, leading to $\tau_{1/2} \sim 69 \pm 4$ min at 23 °C. The ^1H NMR data for **4b** and **10b** are presented in Tables I–III. The UV spectrum of DHP-**10b** was as follows: λ_{max} (methanol) 234 nm (ϵ 16 600), 274 nm (ϵ 13 900); λ_{max} (hexanes) 236 nm (ϵ 14 000), 272 nm (ϵ 11 400).

(B) *tert*-Butyl Schiff Base **4c**. The Schiff base **4c** was prepared from *tert*-butylamine and 13-*cis*-**4a** by the same method used for preparing **4b** (method A). The ^1H NMR spectral data for **4c** in C_6D_6 and in CDCl_3 are given in Tables I and II, respectively. The UV spectrum of **4c** was as follows: λ_{max} (methanol) 228 nm (ϵ 18 700), 256 nm (ϵ 17 700), 344 nm (ϵ 22 900); λ_{max} (hexanes) 224 nm (ϵ 18 900), 250 nm (ϵ 16 600), 336 nm (ϵ 23 400). Unlike in the preparation of the *n*-butyl Schiff base **4b**, the sample of **4c** was uncontaminated by cyclized material (i.e., **10c**). Brief heating of **4c** in C_6D_6 for 15 min led to the appearance of new geometric isomers (judged by the appearance of two new doublets in the region δ 8–8.5) and the appearance of what is presumed to be DHP-**10c** (judged by the appearance of two new doublets at δ 4.8 and 5.0, similar to the corresponding H_{11} and H_{14} signals of the *n*-butyl DHP-**10b**). The thermolysis of **4c** was not investigated further.

Schiff Bases of 12,20-Tetramethylene-11,13-*dicis*-retinal (6a). (A) *n*-Butyl Schiff Base **6b** and DHP-**10b**. The Schiff base **6b** was prepared from 11,13-*dicis* aldehyde **6a** as usual from *n*-butylamine by method A. Its ^1H NMR spectral data are summarized in Tables I and II. The Schiff base **6b** exhibited atropisomerism as evidenced by the appearance of the α -methylene hydrogens next to the nitrogen of the *n*-butyl group as a pair of multiplets at δ 3.40 and 3.54 (indicated as the signal at δ 3.45 in Table I). Unlike the *n*-butyl Schiff base 13-*cis*-**4b** (which was already ~50% cyclized to DHP-**10b** at the time its ^1H NMR spectrum was first recorded after its preparation), the ^1H NMR spectrum of **6b** was quite free

of signals due to **10b**. Upon heating **6b** in C_6D_6 , monitoring of the signals at δ 3.45 (2 H, assigned to the α -methylene hydrogens of **6b** as indicated above) and the pair of doublets at δ 4.69 and 4.77 (2 H, assigned to H_{14} and H_{11} of DHP-**10b**) leads to a half-life for cyclization of **6b** to **10b** of $\tau_{1/2} \sim 10 \pm 3$ min at 78 °C. Thus, like the faster cyclization to **7b** of 13-*cis* Schiff base **3b** ($\tau_{1/2} \sim 11$ min at 23 °C) compared to the corresponding 11,13-*dicis* Schiff base **5b** ($\tau_{1/2} \sim 4$ min at 78 °C), the less hindered 13-*cis*-**4b** ($\tau_{1/2} \sim 70$ min at 25 °C) cyclized to **10b** faster than did 11,13-*dicis*-**6b** ($\tau_{1/2} \sim 10$ min at 78 °C) to the same **10b**. The UV spectrum of 11,13-*dicis*-**6b** was as follows: λ_{max} (MeOH) 238 nm (ϵ 10 000), 296 nm (ϵ 8200); λ_{max} (hexanes) 232 nm (ϵ 9700), 296 nm (ϵ 7900). The UV spectrum of cyclized DHP-**10b** was presented above.

(B) *tert*-Butyl Schiff Base **6c**. Schiff base **6c** was prepared from **6a** and *tert*-butylamine by the usual method A. The ^1H NMR spectral data are presented in Tables I (C_6D_6) and II (CDCl_3). Like the corresponding *n*-butyl Schiff base **6b**, the ^1H NMR spectrum of *tert*-butyl Schiff base **6c** was quite clean. Thermal studies were not carried out with this substance. The UV spectrum of **6c** was as follows: λ_{max} (MeOH) 228 nm (ϵ 13 300), 296 nm (ϵ 9300); λ_{max} (hexanes) 228 nm (ϵ 10 600), 306 nm (ϵ 8500).

Schiff Bases of Parent 9-*cis*-Retinal (11b and 11c). Method A was utilized to transform 9-*cis*-retinal (**11a**, sample prepared by oxidation of the corresponding retinol provided by the Hoffmann-La Roche Co.) to the corresponding *n*-butyl (**11b**) and *tert*-butyl Schiff bases (**11c**). The ^1H NMR data obtained in C_6D_6 are summarized in Table I. For the thermolysis of **11b** (see the time course given in Figure 8A), the ^1H NMR signals assigned to H_{15} (Schiff base C–H) in the region $\delta > 8.0$ were monitored (only three doublets appeared), and the assignments were as follows: δ 8.20 (9-*cis*-**11b**), 8.25 (*all-trans*-**1b**), and 8.48 (9,13-*dicis*-**13b**). It is uncertain whether the latter signal at δ 8.48 can be attributed to a mixture of 9,13-*dicis*-**13b** plus 13-*cis*-**2b** (whose H_{15} signal appears at δ 8.52 as indicated in Table I) or to 9,13-*dicis*-**13b** alone as indicated in Figure 8A. However, thermolysis of the *tert*-butyl Schiff base **11c** (see Figure 8B for the time course) revealed the presence of a fourth minor component in the region near δ 8.5 (i.e., the two doublets near δ 8.5 could be assigned to 13-*cis*-**2c** and 9,13-*dicis*-**13c**), and again the reaction was monitored by integrating all four of the doublet signals appearing in the region $\delta > 8.0$. The assignments were as follows: δ 8.31 (9-*cis*-**11c**), 8.37 (*all-trans*-**1c**), 8.61 (13-*cis*-**2c**), and 8.62 (9,13-*dicis*-**13c**). The results were complementary to those shown in Figure 7 as discussed in the text.

Schiff Bases of Parent 11-*cis*-Retinal (12b and 12c). The *n*-butyl (**12b**) and *tert*-butyl Schiff bases (**12c**) of 11-*cis*-retinal (**12a**, sample provided by the Hoffmann-La Roche Co.) were prepared with method A, and their ^1H NMR spectra (C_6D_6) were obtained (see Table I) for reference purposes. For the thermolysis of the Schiff bases of *all-trans*-**1**, 13-*cis*-**2**, and 9-*cis*-**11** as described above, signals assignable to the 11-*cis* isomer could not be detected.

***n*-Butyl Schiff Base of 12,20-Tetramethylene-9,11,13-*tricis*-retinal (14b), Its 9,13-*Dicis* Isomer (16b), and 9-*cis*-DHP-15b.** Since 12-*s-cis*-locked 9,11,13-*tricis* aldehyde **14a** was also available,^{13h} we also prepared (using method A as usual) and briefly examined the thermal behavior of *n*-butyl Schiff base **14b**. The ^1H NMR spectrum of the latter in C_6D_6 was as follows: δ 0.91 (3 H, CH_3 of *n*-butyl side chain, t, $J \sim 7.4$ Hz), 1.14 (6 H, ring *gem*-dimethyl, s), 1.84 and 1.94 (2×3 H, allylic CH_3 's, two s), 3.35 and 3.50 [2 H, diastereotopic hydrogens of CH_2 α to nitrogen of *n*-butyl group (nonequivalency due to atropisomerism as for **6b**), two m], 6.26 (1 H, H_{10} or H_{11} , d, $J \sim 11.6$ Hz), 6.34 (1 H, H_8 , d, $J \sim 16.0$ Hz), 6.51 (1 H, H_{14} , d, $J \sim 9.3$ Hz), 6.74 (1 H, H_{11} or H_{10} , d, $J \sim 11.6$ Hz), 7.02 (1 H, H_7 , d, $J \sim 16.0$ Hz), 8.11 (1 H, H_{15} , d, $J \sim 9.2$ Hz). In CDCl_3 , the sample exhibited the following: δ 0.89 (3 H, CH_3 of *n*-butyl side chain, t, $J \sim 7.4$ Hz), 1.05 (6 H, ring *gem*-dimethyl, s), 1.77 and 1.88 (2×3 H, allylic CH_3 's, two s), 3.29 and 3.45 (2 H, diastereotopic hydrogens of CH_2 α to nitrogen as above, two m), 5.86 (1 H, H_{10} and H_{11} , d, $J \sim 11.6$ Hz), 6.14 (1 H, H_{14} , d, $J \sim 9.0$ Hz), 6.17 (1 H, H_8 , d, $J \sim 16.0$ Hz), 6.51 (1 H, H_{11} or H_{10} , d, $J \sim 11.6$ Hz), 6.65 (1 H, H_7 , d, $J \sim 16.0$ Hz), 7.76 (1 H, H_{15} , d, $J \sim 9.0$ Hz). The UV spectra were as follows: λ_{max} (hexanes) 232 nm (ϵ 19 500), 304 nm (ϵ 18 200); λ_{max} (methanol) 236 nm, 302 nm.

The ^1H NMR sample of **14b** in C_6D_6 was heated at 78 °C for 30 min, resulting in its essentially complete, clean transformation to 9-*cis*-DHP-**15b**. The ^1H NMR spectrum in C_6D_6 exhibited the following: δ 0.83 (3 H, t, $J \sim 7.4$ Hz), 1.15 (6 H, ring *gem*-dimethyl, s), 1.84 and 1.92 (2×3 H, allylic methyls, two s), 2.67 (1 H, first diastereotopic hydrogen α to nitrogen of *n*-butyl group, ddd, $J \sim 13.6$, 7.4, and 7.4 Hz), 3.01 (1 H, second diastereotopic hydrogen α to nitrogen of *n*-butyl group, ddd, $J \sim 13.6$, 6.9, and 6.9 Hz), 4.79 (1 H, H_{11} , d, $J \sim 7.1$ Hz), 4.92 (1 H, H_{14} , d, $J \sim 10.1$ Hz), 5.82 (1 H, H_{10} , d, $J \sim 7.1$ Hz), 6.08 (1 H, H_{15} , d, $J \sim 10.1$ Hz), 6.40 (1 H, H_8 , d, $J \sim 16.2$ Hz), 6.82 (1 H, H_7 , d, $J \sim 16.2$ Hz). The UV spectrum revealed the following: λ_{max} (MeOH) 272 nm (ϵ 11 900), 234 nm (ϵ 15 100).

The corresponding 9,13-dicis aldehyde **16a** was also reacted with *n*-butylamine according to method A. The initial ^1H NMR spectrum in C_6D_6 revealed the presence of the same 9-*cis*-DHP-**15b** (>80%) admixed with <20% of what is presumably 9,13-dicis Schiff base **16b** (H_{15} doublet, $J \sim 9$ Hz, at δ 8.4). After 30 min at room temperature, only a trace of **16b** remained, and the latter was completely absent after 90 min wherein the ^1H NMR spectrum of the resulting 9-*cis*-DHP-**15b** was identical with that produced from 9,11,13-*tricyclic*-**14b**.

Dihydropyridinium Salt 19 by Protonation of DHP-7b in CD_2Cl_2 . DHP-**7b** was prepared in the usual way from **3a** and *n*-butylamine according to method A. The vacuum-dried DHP-**7b** was dissolved in CD_2Cl_2 , and its ^1H NMR spectrum was recorded (300 MHz; residual protonated CD_2Cl_2 as internal standard at δ 5.33): δ 1.010 (9 H, *t*-Bu, s), 1.007 (6 H, $2\text{C}_1\text{-Me}$, s), 1.70 (3 H, 3 H_{18} , s), 1.81 (3 H, 3 H_{19} , d, $J \sim 1.1$ Hz), 2.77 (1 H, first diastereotopic hydrogen α to nitrogen of *n*-Bu, ddd, $J \sim 13.9$, 8.0, and 6.4 Hz), 2.95 (1 H, second diastereotopic hydrogen α to nitrogen of *n*-Bu, ddd, $J \sim 13.9$, 8.0, and 6.4 Hz), 4.61 (1 H, H_{14} , dd, $J \sim 7.5$ and 2.1 Hz), 4.66 (1 H, H_{12} , dd, $J \sim 5.0$ and 2.1 Hz), 4.81 (1 H, H_{11} , dd, $J \sim 9.4$ and 5.0 Hz), 5.75 (1 H, H_{10} , d, $J \sim 9.4$ Hz), 5.96 (1 H, H_{15} , d, $J \sim 7.5$ Hz), 5.98 (1 H, H_8 , d, $J \sim 16.2$ Hz), 6.10 (1 H, H_7 , d, $J \sim 16.2$ Hz). This spectrum is similar to that recorded in CDCl_3 and C_6D_6 (Table III). The solution of **7b** in CD_2Cl_2 was treated with excess trifluoroacetic acid at ambient temperature, and then the ^1H NMR spectrum was again recorded, indicating the formation of what has been identified as dihydropyridinium salt **19**: δ 1.00 and 0.99

(6 H, $\text{C}_1\text{-Me}_2$, two s), 1.17 (9 H, *t*-Bu, s), 1.66 (3 H, 3 H_{18} , s), 1.97 (3 H, 3 H_{19} , d, $J \sim 1.0$ Hz), 2.60 (1 H, first diastereotopic H_{12} , dd, $J \sim 18.7$ and 4.2 Hz), 3.00 (1 H, second diastereotopic H_{12} , dd, $J \sim 18.7$ and 4.8 Hz), 3.7 (2 H, CH_2 α to nitrogen, m), 4.80 (1 H, H_{11} , ddd, $J \sim 9.9$, 4.8, and 4.2 Hz), 5.42 (1 H, H_{10} , d, $J \sim 9.9$ Hz), 5.98 (1 H, d, $J \sim 16.1$ Hz), 6.4 (2 H, H_7 and H_{14} , m), 8.4 (1 H, H_{15} , br m).

Acknowledgment. This study was supported by NIH Grant DK-16595. We acknowledge NATO for a postdoctoral fellowship to A.R.d.L. The Hoffmann-La Roche Co., Nutley, NJ, and Badische-Anilin und Soda Fabrik, Ludwigshafen, West Germany, are also acknowledged for providing starting materials utilized in this study.

Registry No. **1a**, 116-31-4; **1b**, 61769-47-9; **1c**, 92216-32-5; **2a**, 472-86-6; **2b**, 68737-92-8; **2c**, 92098-20-9; **3a**, 106190-63-0; **3b**, 115018-97-8; **3c**, 115019-02-8; **4a**, 90736-88-2; **4b**, 115018-99-0; **4c**, 115019-04-0; **5a**, 113775-89-6; **5b**, 115075-01-9; **5c**, 115075-02-0; **6a**, 85236-10-8; **6b**, 115019-01-7; **6c**, 120120-49-2; (\pm)-**7b**, 115018-98-9; (\pm)-**7c**, 115019-03-9; (\pm)-**9b**, 115031-66-8; (\pm)-**9c**, 120120-50-5; (\pm)-**10b**, 115019-00-6; (\pm)-**10c**, 120120-51-6; **11a**, 514-85-2; **11b**, 68737-94-0; **11c**, 114127-33-2; **12a**, 564-87-4; **12b**, 68737-93-9; **12c**, 114128-95-9; **13a**, 23790-80-9; **13b**, 120201-10-7; **13c**, 120201-11-8; **14a**, 85236-12-0; **14b**, 120120-46-9; (\pm)-**15b**, 120120-47-0; **16a**, 90745-29-2; **16b**, 120120-48-1; **17**- CF_3CO_2^- , 120120-42-5; **18**- CF_3CO_2^- , 120120-43-6; **19**- CF_3CO_2^- , 120120-45-8.

A Spectroscopic, Photocalorimetric, and Theoretical Investigation of the Quantum Efficiency of the Primary Event in Bacteriorhodopsin

Robert R. Birge,* Thomas M. Cooper, Albert F. Lawrence, Mark B. Masthay, Christ Vasilakis, Chian-Fan Zhang, and Raphael Zidovetzki

Contribution from the Department of Chemistry and Center for Molecular Electronics, Syracuse University, Syracuse, New York 13244. Received July 15, 1988

Abstract: The spectroscopic, photochemical, and energetic properties of the primary event of light-adapted bacteriorhodopsin (bR) are investigated with pulsed laser cryogenic photocalorimetry, photostationary-state spectral analysis, INDO-PSDCI molecular orbital theory, and semiempirical molecular dynamics theory. The principal goal is to explore the photophysical origins of the controversy concerning the primary quantum yield. The ratio of the forward to reverse quantum yields (Φ_1/Φ_2) of bR is observed to equal 0.45 ± 0.03 at 77 K in glycerol/water solution. Thus, Φ_1 must be less than 0.48 under these experimental conditions. The mole fraction of K (χ_K^{500}) in the 77 K, 500-nm photostationary state is observed to equal 0.46 ± 0.04 . The calculated absorption spectrum of K at 77 K has a maximum absorbance at 620 nm and a molar absorptivity at λ_{max} of $63\,900\text{ M}^{-1}\text{ cm}^{-1}$. The oscillator strength associated with excitation into the λ_{max} band f_K is determined to be 0.95 on the basis of log-normal regression analysis. The corresponding values for bR at 77 K are $\lambda_{\text{max}} = 577\text{ nm}$, $\epsilon_{\text{max}} = 66\,100\text{ M}^{-1}\text{ cm}^{-1}$, and $f_{\text{bR}} = 0.87$. The observation that $f_K > f_{\text{bR}}$ is consistent with the displacement of the $\text{C}_{15}=\text{NH}$ portion of the retinyl chromophore away from a negatively charged counterion as a consequence of the all-trans to 13-*cis* photoisomerization. It is difficult to reconcile the observation that $f_K > f_{\text{bR}}$ with the proposal that the primary event involves an all-trans to 13-*cis*,14-*s-cis* photoisomerization, because the latter geometry is predicted to have a significantly lower λ_{max} band oscillator strength relative to that of the all-trans precursor. Experimental and theoretical evidence is presented which suggests that two distinct forms of light-adapted bacteriorhodopsin may exist. We propose that these two forms have characteristic photocycles with significantly different primary quantum yields. INDO-PSDCI molecular orbital procedures and semiempirical molecular dynamics simulations predict that one ground-state geometry of bR undergoes photochemistry with a quantum yield Φ_1 of ~ 0.27 and that a second ground-state geometry, with a slightly displaced counterion, yields $\Phi_1 \sim 0.74$. This theoretical model may explain the observation that literature measurements of Φ_1 tend to fall into one of two categories—those that observe $\Phi_1 \sim 0.33$ or below and those that observe $\Phi_1 \sim 0.6$ or above. The observation that all photostationary-state measurements of the primary quantum yield give values near 0.3 and all direct measurements of the quantum yield result in values near 0.6 suggests that photochemical back-reactions may select the bacteriorhodopsin conformation with the lower quantum yield. We conclude that the primary photoproduct K has an enthalpy $15.9 \pm 3.2\text{ kcal mol}^{-1}$ larger than that of bR at 77 K in agreement with our previous assignment (Birge, R. R.; Cooper, T. M. *Biophys. J.* **1983**, *42*, 61–69). However, we anticipate that this energy storage measurement is not necessarily valid for those environments yielding much higher quantum yields (e.g., $\Phi \geq 0.6$), and we suggest that energy storage in the latter situation is not only smaller but is likely to be insufficient to pump two protons under nominal *in vivo* conditions. The two photocycles may have developed as a natural biological requirement that *Halobacterium halobium* have the capacity to adjust the efficiency of the photocycle in relation to the intensity of light and/or membrane electrochemical gradient.

Bacteriorhodopsin is the light-harvesting protein of the purple membrane of the halophilic microorganism *Halobacterium halobium*.^{1–5} The light-adapted form of this protein undergoes a

complex photocycle (Figure 1) which transports one (or more) proton(s) across the membrane.⁶ The primary structure of this protein is known,^{7,8} and this information, along with spectroscopic